สมรรถนะของท่อคาร์บอนระดับนาโนเมตรที่ปรับแต่งด้วยนิกเกิลโดยมีรูทีเนียมเป็นโปรโมเตอร์ในปฏิกิริยาไฮโดรเทอร์มอลแก๊สซิฟิเคชันของกลูโคส

นายภูมิกวี ช่างเขียนดี

วิทยานิพนธ์นี้เป็นส่วนหนึ่งของการศึกษาตามหลักสูตรปริญญาวิศวกรรมศาสตรมหาบัณฑิต
สาขาวิชาวิศวกรรมเคมี ภาควิชาวิศวกรรมเคมี
คณะวิศวกรรมศาสตร์ จุฬาลงกรณ์มหาวิทยาลัย
ปีการศึกษา 2559

PERFORMANCE OF CNT MODIFIED BY NI WITH RU AS PROMOTER IN HYDROTHERMAL GASIFICATION OF GLUCOSE

Mr. Poomkawee Changkiendee

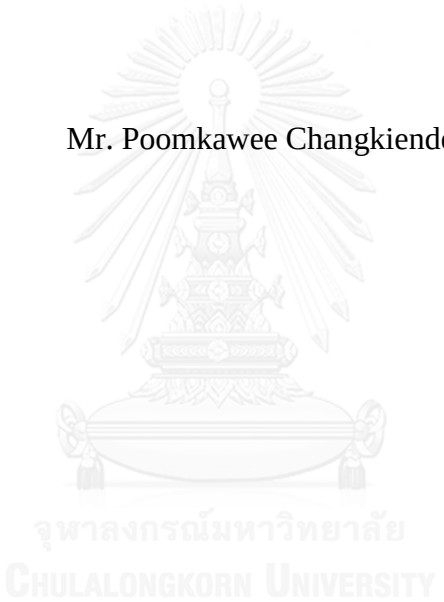

A Thesis Submitted in Partial Fulfillment of the Requirements
for the Degree of Master of Engineering Program in Chemical Engineering
Department of Chemical Engineering
Faculty of Engineering
Chulalongkorn University
Academic Year 2016

Thesis Title	PERFORMANCE OF CNT MODIFIED BY NI WITH RU AS PROMOTER IN HYDROTHERMAL GASIFICATION OF GLUCOSE
By	Mr. Poomkawee Changkiendee
Field of Study	Chemical Engineering
Thesis Advisor	Associate Professor Tawatchai Charinpanitkul, D.Eng.
Thesis Co-Advisor	Chalita Ratanatawanate, Ph.D.

Accepted by the Faculty of Engineering, Chulalongkorn University in Partial Fulfillment of the Requirements for the Master's Degree

.....Dean of the Faculty of Engineering
(Associate Professor Supot Teachavorasinskun, D.Eng.)

THESIS COMMITTEE

.....Chairman
(Varun Taepaisitphongse, Ph.D.)

.....Thesis Advisor
(Associate Professor Tawatchai Charinpanitkul, D.Eng.)

.....Thesis Co-Advisor
(Chalita Ratanatawanate, Ph.D.)

.....Examiner
(Akawat Sirisuk, Ph.D.)

.....External Examiner
(Assistant Professor Thongthai Witoon, Ph.D.)

ภูมิกวี ช่างเขียนดี : สมรรถนะของท่อคาร์บอนระดับนาโนเมตรที่ปรับแต่งด้วยนิกเกิลโดยมีรูทีเนียมเป็นโปรโมเตอร์ในปฏิกิริยาไฮโดรเทอร์มอลแก๊สซิฟิเคชันของกลูโคส (PERFORMANCE OF CNT MODIFIED BY NI WITH RU AS PROMOTER IN HYDROTHERMAL GASIFICATION OF GLUCOSE) อ.ที่ปรึกษาวิทยานิพนธ์หลัก: รศ. ดร.ธวัชชัย ชรินพาณิชกุล, อ.ที่ปรึกษาวิทยานิพนธ์ร่วม: ชลิตา รัตนเทวะเนตร, 62 หน้า.

กระบวนการผลิตแก๊สในน้ำที่สภาวะวิกฤติยิ่งยวดเป็นกระบวนการที่มีประสิทธิภาพในการผลิตแก๊สให้ได้ในปริมาณที่มาก ในงานวิจัยนี้กลูโคสถูกนำมาเป็นสารตั้งต้นในการผลิตแก๊สในน้ำที่สภาวะวิกฤติยิ่งยวดที่อุณหภูมิและความดัน 400 องศาเซลเซียสและ 25 เมกะปาสคาล ตามลำดับ โดยใช้เตาปฏิกรณ์แบบกะ ตัวเร่งปฏิกิริยานิกเกิลที่ฝังบนท่อคาร์บอนที่มีผนังชั้นเดียวระดับนาโนเมตร (Ni/SWCNT) และตัวเร่งปฏิกิริยานิกเกิลและรูทีเนียมที่ฝังบนท่อคาร์บอนที่มีผนังชั้นเดียวระดับนาโนเมตร (Ru-Ni/SWCNT) รวมถึงท่อคาร์บอนที่มีผนังชั้นเดียวระดับนาโนเมตร (SWCNT) ได้ถูกนำมาใช้ทดสอบประสิทธิภาพในการทดลองนี้ ความเข้มข้นของกลูโคสคือ 5 เปอร์เซ็นต์โดยมวล อัตราส่วนโดยมวลระหว่างตัวเร่งปฏิกิริยาต่อกลูโคสคือ 3/10 ระยะเวลาในการทำปฏิกิริยาคือ 15 30 และ 60 นาที เครื่องมือวิเคราะห์ประกอบด้วย EDX BET และ XRD ยืนยันความสำเร็จของการสังเคราะห์ตัวเร่งปฏิกิริยา ผลิตภัณฑ์ของเหลว แก๊ส และของแข็งเป็นผลิตภัณฑ์หลักที่ได้ในแต่ละการทดลอง Ni/SWCNT และ Ru-Ni/SWCNT ผลิตแก๊สในปริมาณสูงเมื่อเทียบกับ SWCNT และการไม่ใช้ตัวเร่งปฏิกิริยา อย่างไรก็ตามผลได้ของไฮโดรเจนค่อยๆ เพิ่มขึ้นเมื่อใช้ SWCNT มีเทนถูกผลิตได้เพิ่มสูงขึ้นเมื่อมีการใส่นิกเกิลหรือรูทีเนียมด้วยเช่นกัน ปฏิกิริยาการเปลี่ยนน้ำเป็นแก๊สและปฏิกิริยาการผลิตมีเทนเป็นปฏิกิริยาหลักต่อการเกิดไฮโดรเจนและมีเทนตามลำดับ นอกจากนี้ยังพบสิ่งที่น่าสนใจอีกคือปฏิกิริยาต่างๆดำเนินไปอย่างรวดเร็วมากในช่วงเวลา 15 นาทีแรก ในช่วงนี้กลูโคสจะสลายตัวอย่างรวดเร็วและเกิดเป็นสารอนุพันธ์ต่างๆ ไม่ว่าจะเป็น เฟอร์ฟูรัล และ 5-ไฮดรอกซีเมทิลเฟอรีฟูรัล รวมถึงผลิตภัณฑ์ของเหลวต่างๆ อย่างไรก็ตามผลิตภัณฑ์ของแข็งได้ถูกผลิตขึ้นอย่างรวดเร็วจาก เฟอร์ฟูรัล และ 5-ไฮดรอกซีเมทิลเฟอรีฟูรัล เป็นผลทำให้เกิดการลดลงของผลได้ของแก๊สไฮโดรเจนและมีเทนเมื่อเวลาในการทำปฏิกิริยายาวนานขึ้น

ภาควิชา วิศวกรรมเคมี	ลายมือชื่อนิสิต .....
สาขาวิชา วิศวกรรมเคมี	ลายมือชื่อ อ.ที่ปรึกษาหลัก .....
ปีการศึกษา 2559	ลายมือชื่อ อ.ที่ปรึกษาร่วม .....

5770270621 : MAJOR CHEMICAL ENGINEERING
KEYWORDS: SUPERCRITICAL WATER GASIFICATION / GLUCOSE / SINGLE WALLED-CARBON NANOTUBE / NICKEL / RUTHENIUM

POOMKAWEE CHANGKIENDEE: PERFORMANCE OF CNT MODIFIED BY NI WITH RU AS PROMOTER IN HYDROTHERMAL GASIFICATION OF GLUCOSE. ADVISOR: ASSOC. PROF. TAWATCHAI CHARINPANITKUL, D.Eng., CO-ADVISOR: CHALITA RATANATAWANATE, Ph.D., 62 pp.

Supercritical water gasification (SCWG) is a promising way to produce energy from biomass in term of gaseous product. In this study, glucose was gasified in supercritical water in a batch reactor at temperature of 400 °C and pressure of 25 MPa. Nickel supported-single walled carbon nanotube (Ni/SWCNT), Ni/SWCNT promoted with ruthenium (Ru-Ni/SWCNT), and single walled carbon nanotube (SWCNT) were employed to study the effect of each catalyst on gasification product. Concentration of glucose was 5 wt%. Ratio of catalyst to glucose was 3:10 by weight. Reaction time was varied from 15 to 60 min. Energy dispersive X-ray spectroscopy (EDX), Brunauer–Emmett–Teller (BET) analysis, and X-ray diffraction (XRD) were used to confirm the catalyst synthesis achievement. After SCWG, gaseous, liquid, and solid (char) products were observed. Ni/SWCNT and Ru-Ni/SWCNT highly increased gas yield when compared to the conditions of SWCNT and non-catalytic gasification. However, hydrogen yield slightly increased with SWCNT. Methane production was also enhanced by adding metal catalysts, which was attributed that water-gas shift reaction and methanation play an important roles in gaseous phase reaction. Interestingly, it was found that an important period of reaction took place in the first 15 min. At this stage, glucose rapidly decomposed into several intermediates including furfural, 5-(hydroxymethyl)furfural, and other liquid products. However, char was rapidly produced with consumption of furfural and 5-(hydroxymethyl)furfural, resulting in a decrease in hydrogen and methane yield with a longer reaction time.

Department:	Chemical Engineering	Student's Signature	.....
Field of Study:	Chemical Engineering	Advisor's Signature	.....
Academic Year:	2016	Co-Advisor's Signature	.....

ACKNOWLEDGEMENTS

I would like to thank Chulalongkorn University, Hiroshima University, National Nanotechnology Center (NANOTEC), Thailand Graduate Institute of Science and Technology (TGIST) for all the contribution to this research to be successfully accomplished.

Firstly, I would like to give my kind gratitude to Assoc. Prof. Tawatchai Charinpanitkul who has advised me and provided me many opportunities, including introducing me to Hiroshima University and National Nanotechnology Center and teaching many lessons in doing my research and in living as a successful person. Moreover, I would like to give my thankfulness to my co-advisor, Dr. Chalita Ratanatavanate, who has taught me many things related to this research, assisted me to use many analytical instrument in NANOTEC, and gave me an opportunity to receive scholarship from TGIST.

Secondly, I kindly thank scholarship from Hiroshima University which provided me tuition fee when I conducted a part of my research in Faculty of Engineering, Division of Energy and Environmental Engineering. Furthermore, I would like to thank Prof. Yukihiko Matsumura who has advised me and gave a lot of experience when I have conducted my research in his laboratory, named Thermal Laboratory. Moreover, I have got to thank every Thai and Japanese students who have assisted regarding to living in Japan, inviting me to many activities, and assisting me in doing my research.

Thirdly, I would like to thank Thailand Graduate Institute of Science and Technology (TGIST) which has provide me a scholarship including tuition fee, living stipend, and self-developing expense.

Fourthly, I would like to thank Chulalongkorn University. This place has afforded me convenience in doing research and socialization.

Lastly, I would like to thank NANOTEC which allowed me to analyze my samples with High-performance liquid chromatography (HPLC), X-ray diffraction (XRD), and Transmission electron microscopy (TEM).

CONTENTS

Page

Page

List of Tables

Table **Page**

List of Figures

Figure **Page**

CHAPTER I

INTRODUCTION

Fossil fuel has been utilized as conventional source of energy production via conventional method. It can be referred to 3 forms including natural gas, oil or petroleum, and coal. They basically took many hundreds of millions of years to form. Due to an increase in fossil fuel depletion, many researchers have been trying to produce energy from other resources which are renewable and sustainable. Global warming or greenhouse effect is another impact issue which has attracted many concerns toward increment of greenhouse gases. Fossil fuel has been claimed to be the cause of global warming due to its much release of greenhouse gases, such as carbon dioxide (CO_2) and methane (CH_4). Therefore, use of renewable and sustainable sources for energy production can reduces use of fossil fuel.

Utilizing biomass feedstock has received many attentions because it is renewable and sustainable. It contains large amount of carbon, oxygen, and hydrogen in their structure which can be converted into many forms of energy, including solid, liquid and gas. Among conversion techniques, thermochemical conversion technologies, which apply heat to the feedstock, can break down their bonds and to chemically change the original big molecules of the feedstock into many smaller molecules consisting of useful chemicals, liquid fuel, char, and gases.

Supercritical water gasification (SCWG), a technique which employs water at temperature and pressure above its critical point (critical temperature = 374 °C and critical pressure = 22.1 MPa), is a promising method to efficiently convert lignocellulosic feedstock into gaseous product mainly consisting of CO_2, carbon monoxide (CO), hydrogen (H_2), and other small hydrocarbons such as CH_4, ethylene (C_2H_4) and ethane (C_2H_6). CH_4 and CO can be used as syngas to directly produce energy via burning while H_2 can be used in hydrogen cell. H_2 is a clean energy

because it can produce energy without any pollution as by-product. Those gases can be used in many applications as reactant in various reactions [1].

However, high operating temperature of above 600 °C is needed in order to gasify feedstock into gaseous product completely. To avoid such severe conditions of SCWG of biomass, catalyst is mostly introduced in order to obtain high conversion and yield of gaseous product at milder condition. Water can act as reaction medium and also reactant in some reactions whereas catalysts enhance efficiency and consequently increase gaseous yield. It should be noted that selectivity is also an important criterion for choosing catalysts.

Catalyst can provide high conversion of feedstock at relatively mild operating conditions as its catalytic activity. Carbon materials have been investigated as catalyst and catalyst support in SCWG due to their useful characteristics including physical and chemical properties [1-3]. Carbon materials basically have high surface area which can provide large metal dispersion. Thus, high catalytic activity and sintering avoidance can be attained. Furthermore, inertness and chemistry of surface of carbon materials have advantages when they are used as catalyst support. In contrast to silica and alumina, interaction between metal and surface is weak and, thus, undesirable effects of support can be ignored [4]. Some researchers introduced carbon materials for supporting metals and used them to enhance several reactions [2, 5, 6].

There are many metals which their efficiencies have been reportedly investigated toward conversion of biomass feedstock and its model compounds. Nickel (Ni) has been reported as it can enhance yield of hydrogen via water gas-shifted reaction [7-10]. Furthermore, there have many of other metals investigated such as platinum (Pt) and ruthenium (Ru). Ru is precious metal and thus more expensive than Ni catalyst. However, its characteristics have been stated that it could highly converted organic feedstock into chemicals and gaseous product and also promote hydrogen production [5, 6, 11]**.**

There have been many different types of catalysts which are introduced into CSCWG of different biomass species. Nickel (Ni) catalyst has been widely known as

tar-cracking promoter which leads to increase in gaseous product yield. Ni promotes water-gas shift and methanation reactions resulting in H_2 and CH_4 yields, respectively. Hence, H_2 and CH_4 gases are competitively produced. The final yields of H_2 and CH_4 seem to be influenced by the Ni loading when either Ni-supported catalysts or Ni alone is used for CSCWG of biomass feedstock. Meanwhile, Ruthenium (Ru) has been reported that it can break C-C bonds contained in biomass, leading to increase in gaseous product yield.

Glucose and other derivatives of cellulose, hemicellulose, and lignin have been gasified in many researches [12-17], which provide informative results and useful data for determination of biomass conversion. Lignin is known as refractory component against receiving high gas production due to its strong bonding between aromatic compounds. Lignin derivatives mostly further become tarry material through polymerization [18].

1.1 Motivation

As mentioned above, SCWG has been received attention due to its beneficial properties toward gasification of biomass and model compounds into gaseous product. However, high temperature and pressure are needed to completely gasify feedstock in SCWG. In order to reduce severity of SCWG condition, catalyst is typically employed. Carbon based supports have essential properties such as high surface area and high stability. Single walled carbon nanotube (SWCNT) is one of carbon based material that has not been studied widely as catalyst and catalyst support when compared to the others including activated carbon and multi-walled carbon nanotube. Study of catalytic manner of SWCNT as catalyst and catalyst support is of interest. Furthermore, nickel (Ni) metal, which is well-known for its efficiency over gasification process and water-gas shift reaction promotion, is introduced in this work. Still, Ni has drawback that is sintering problem. Therefore, ruthenium (Ru) metal which is precious metal is additionally employed as it has been reported about potential toward organic material conversion improvement. Glucose, which is a model compound of biomass and cellulose, will used as feedstock instead of real biomass to

understand the behavior of glucose gasification under supercritical water without hemicellulose and lignin.

1.2 Objective of research

This research sets its objective to study the effects of nickel (Ni) and ruthenium (Ru) supported on single walled carbon nanotube (SWCNT) for converting glucose to fuel gas by supercritical water gasification.

1.3 Scope of research

1.3.1 Functionalization of SWCNT

- A mixture of equal volume of 8 M sulfuric and 8 M nitric were used to chemically treat SWCNT to produce functionalized single walled carbon nanotube (FSWCNT).

1.3.2 Impregnation of FSWCNT with Ni precursor

- FSWCNT was impregnated with nickel (II) acetate tetra hydrate ($Ni(CH_3COO)_2 \cdot 4H_2O$) as Ni precursor.
- A mixture of Deionized (DI) water and ethanol with volumetric ratio of 9:1 was used.

1.3.3 Impregnation of FSWCNT with Ni and Ru precursor

- FSWCNT was impregnated with $Ni(CH_3COO)_2 \cdot 4H_2O$ and ruthenium (III) chloride hydrate ($RuCl_3 \cdot XH_2O$) as Ni and Ru precursors, respectively.
- A mixture of Deionized (DI) water and ethanol with volumetric ratio of 9:1 was used.

1.3.4 Synthesis of nickel-supported single walled carbon nanotube (Ni/SWCNT) and nickel-supported single walled carbon nanotube promoted with ruthenium (RuNi/SWCNT)

- Catalysts after impregnation proceeded through calcination and reduction respectively.
- Temperature of calcination and reduction was 400 ^{o}C.
- As for calcination, catalysts were heated in nitrogen atmosphere.
- Hydrogen atmosphere was established for reduction process.

1.3.5 Supercritical water gasification (SCWG) of glucose

- SCWG of glucose was performed at temperature of 400 ^{o}C and pressure of 25 MPa.
- Concentration of glucose was 5 wt% in water solution.
- Reaction time was varied from 15-60 min.
- At each reaction time, each catalyst was introduced in SCWG to study effects of each catalyst with reaction time.

CHAPTER II

THEORY AND LITERATURE REVIEW

2.1 Biomass

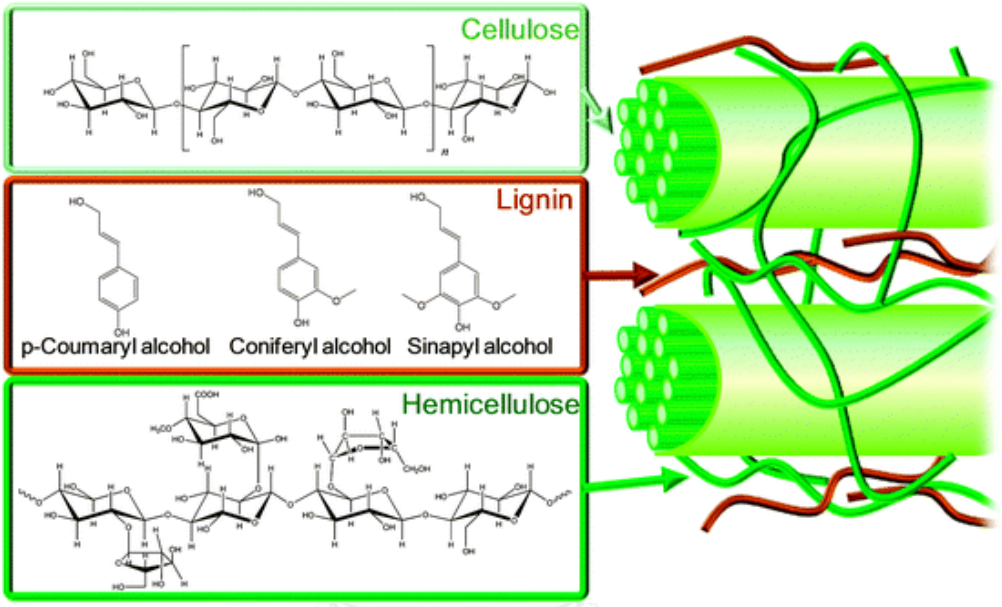

Fig. 2.1 Structure of lignocellulosic biomass [11]

Biomass is an organic material which can be classified into edible and non-edible biomass. Biomass can also be categorized into plant and animal matters and others, depending on what criteria is used for classification. Biomass is naturally a source of energy which absorbs solar energy and stored in plant by photosynthesis process. Lignocellulosic is commonly used as feedstock among all kinds of biomass. It consists of 3 major components as cellulose, hemicellulose, and lignin as shown in Fig. 2.1[11]. These 3 natural polymeric molecules can change into useful chemicals and fuels in forms of solid, liquid, and gas via conversion techniques [19]. Different conversion routes basically lead to different products. Cellulose is a homopolymer of glucose bonded with β-glycosidic bonds. Hemicellulose is a heteropolymer consisting of pentose, hexose, and uronic acid. Lignin is rich in aromatic molecules mainly

consisting of three primary monomers which are p-Coumaryl alcohol, Coniferyl alcohol, and Sinapyl alcohol [19].

2.2 Conversion techniques

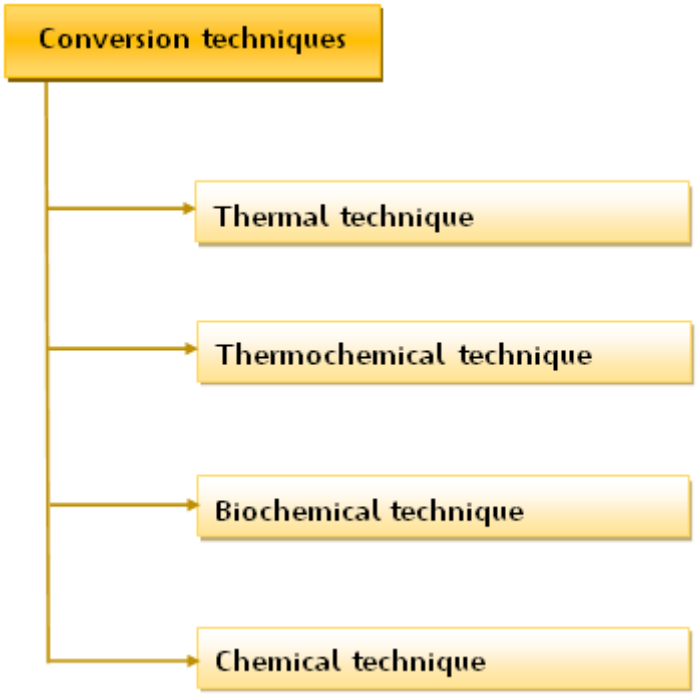

Fig. 2.2 Classifications of biomass conversion techniques

There are many techniques for producing energy from biomass. Basically, they are classified into 4 main technologies including thermal, thermochemical, biochemical, and chemical conversion techniques.

2.2.1 Thermal conversion techniques

- Combustion

Combustion is conversion technique which energy is directly generated by burning biomass in a presence of oxygen in furnaces and boilers. Heat of combustion is converted into steam in boiler. Steam is used to drive turbines and consequently produces electricity and mechanical energy. Heating or cooling system is also processed using steam [19].

- Co-firing

Co-firing is a practical method which biomass and fossil fuel are converted into energy via combustion together. Fossil fuel has been clearly known as high pollution emission after its conversion process in power plant. Pollution can refer to sulfur, CO_2, and greenhouse gases. Introducing biomass in fossil fuel power plant has advantages. Power plant that is located nearby agriculture fields where tons of biomass residues are discharged. Combustion of those residues combined with fossil fuel for energy production can reduce cost effectively due to extremely low cost of biomass residue feedstock [19].

- Co-generation

Co-generation, which is called combined heat and power (CHP), is the concurrent generation of heat and electricity. Heat is by-product when electricity is produced. Heat is typically released to environment through cooling towers or to near-by water sources [19].

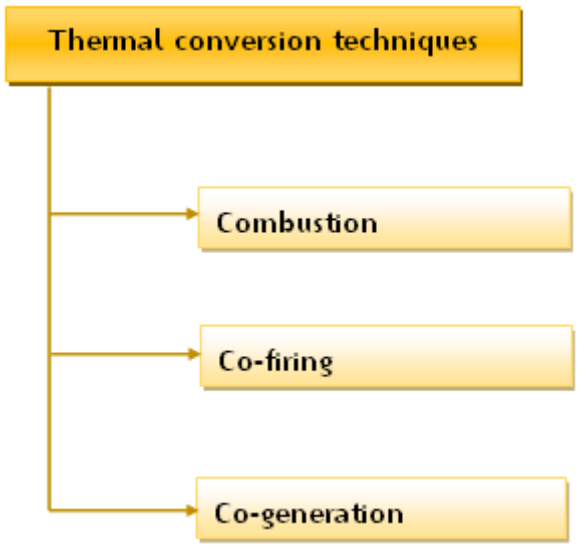

Fig. 2.3 Thermal conversion techniques

2.2.2 Thermochemical conversion technique

- Pyrolysis

Biomass is converted into gaseous, liquid, and solid products under high temperature and inert atmosphere in an absence of oxygen to avoid the complete oxidation of feedstock into massive production of CO2 and water. Small hydrocarbon gases and hydrogen can be produced under inert atmosphere of nitrogen and/or helium. Basically, biomass is not completely gasified into gaseous product. Liquid phase can be observed where tars, oils, and other chemicals are produced because not all of long molecules in biomass are broken into gaseous products but some still remain in liquid and/or solid phases [19].

- Carbonization

Carbonization can refer to a kind of pyrolysis but aiming to produce solid as main product instead of producing liquid and gaseous products. This solid is called charcoal. Carbonization is a very comparably long and slow process compared to pyrolysis. Charcoal can be used for many applications [19].

- Gasification

Gasification needs higher temperature and fast reaction time compared to pyrolysis and carbonization. Heating rate must be very high to avoid the undesirable reactions at relatively low temperature [19].

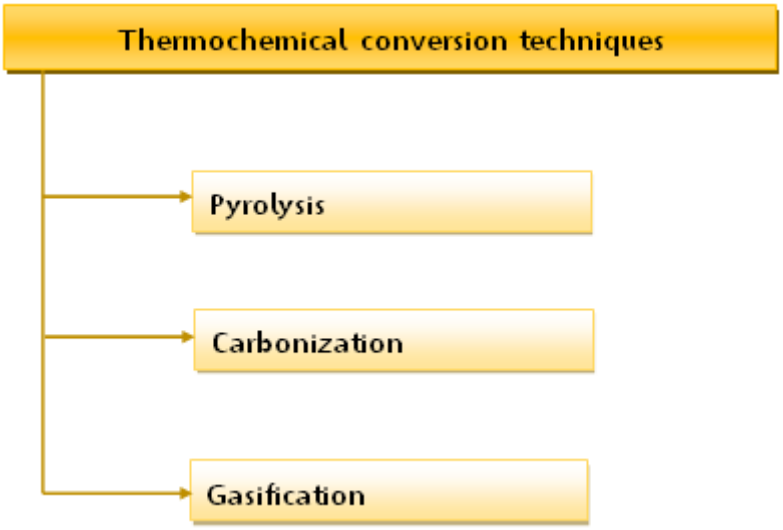

Fig. 2.4 Thermochemical conversion techniques

2.3 Supercritical water gasification

Gasification of biomass in supercritical water is a promising conversion technique in which water is heated up and pressurized until temperature and pressure exceed its critical point. The critical point of pure water is 374 °C and 22.1 MPa. Water at temperature and pressure above its critical point has many advantageous properties on conversion of biomass and organic material into many kinds of products consisting of gas, liquid and solid products [1]. Properties of supercritical water extremely change at temperature and pressure near and above the critical point and were discussed in this chapter.

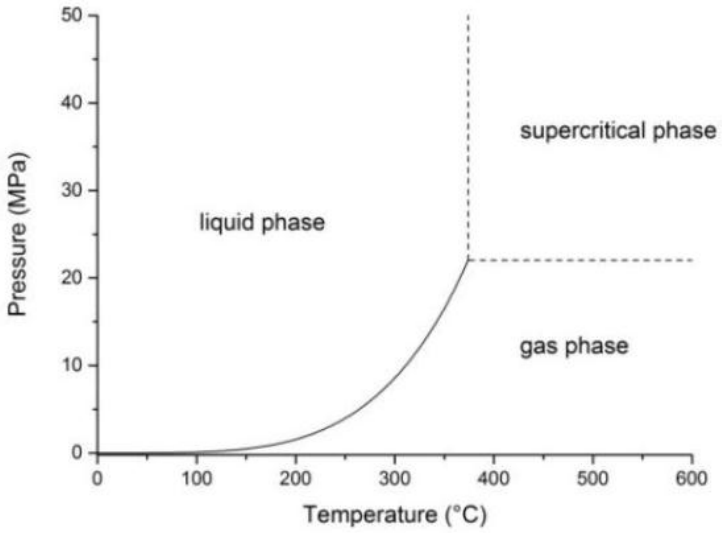

Fig. 2.5 Phase diagram of water [1]

From Fig. 2.6, dielectric constant of water above its critical point drastically decreases and gets close to that of organic material, resulting in improving solubility of organic material in water and, consequently, enhancement of homogeneity of feedstock. Hence, Hindrance of mass transfer between water and biomass feedstock can be negligible. Then, fast and complete reactions can be achieved.

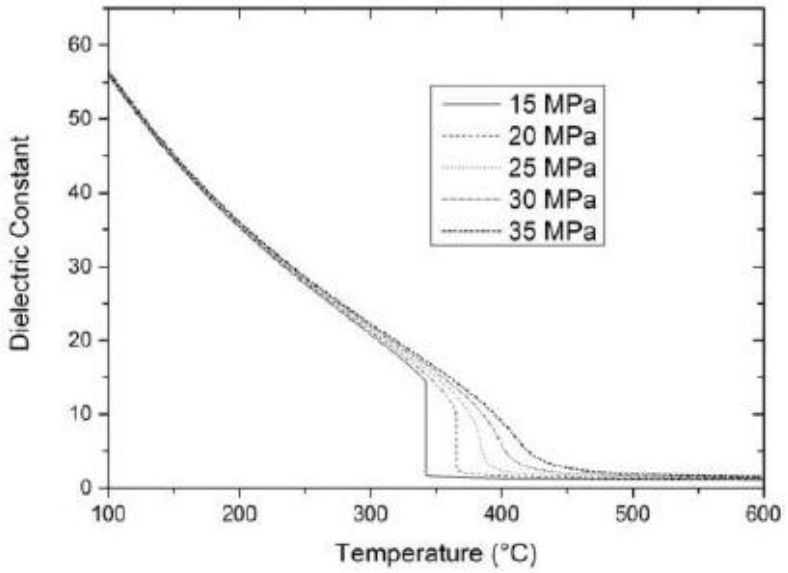

Fig. 2.6 Dielectric constant of water at various temperatures and pressures [1]

From Fig. 2.7, density of water above its critical point decreases significantly but it is still higher than that of steam water. Viscosity of water is similar to gaseous phase, leading to improvement of mass transfer and solvation characteristics.

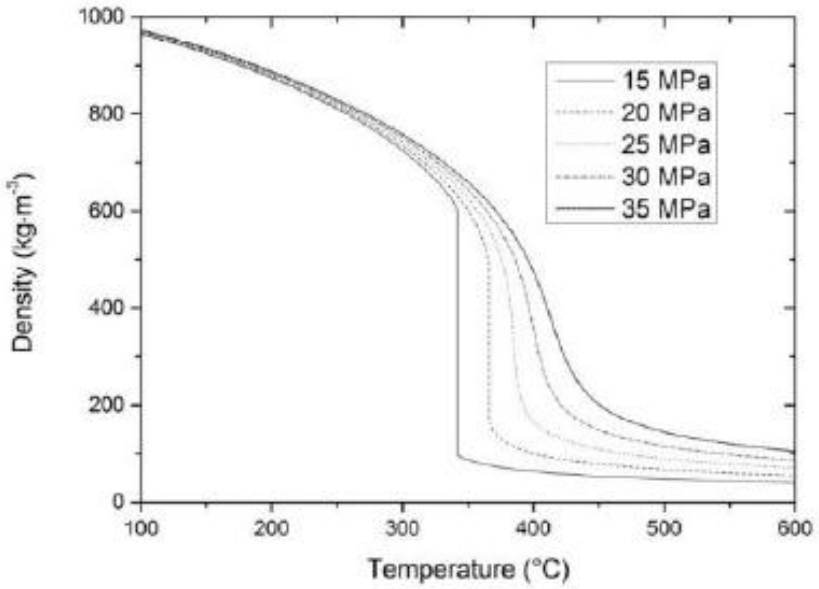

Fig. 2.7 Density of water at various temperatures and pressures[1]

Gasification of biomass using water as medium can be categorized into 2 kinds, consisting of subcritical and supercritical water gasification processes. These 2 kinds can deal with biomass feed stock with high moisture content. Drying process is not needed so that biomass with high moisture content can be directly gasified without additional cost for pre-drying unit. As for subcritical water gasification of biomass, gaseous product yield is lower than that produced from supercritical water gasification due to milder operating condition. Subcritical water gasification employs water at the temperature over normal boiling point (100 °C at 101.325 kPa). In other words, water remains liquid phase at temperature higher than 100 °C and behaves as reaction medium to biomass or organic material to react. Liquid water at temperature above 100 °C can be called hot compressed water which has many advantages toward gasification of biomass or organic material. Under subcritical water condition, biomass is converted into smaller compounds which are mostly in liquid phase [1].

Biomass is basically composed of cellulose, hemicellulose, and lignin. There have been several researchers conducting sub- and supercritical water gasification of their model compounds to avoid the complexity of interpretation [19].

2.4 Heterogeneous catalyst fundamental knowledge

2.4.1 Supporting catalyst

There are 2 types of catalysts consisting of homogeneous and heterogeneous catalysts. Homogeneous catalyst means any catalyst whose phase is the same as reactant or product, which make it hard to be separated from the process. Acidic and basic solutions have been used as homogeneous catalysts for promoting some reactions in hydrothermal process.

Heterogeneous catalyst is referred to any catalyst whose phase is different from reactant or product. Heterogeneous catalyst is frequently mentioned as solid phase catalyst that can be easily separated from the process by, for instance, filtering or drying. Active metal is normally introduced to the support surface in order to improve catalytic activity and performance of catalyst. Selection of catalyst is essential and depends on desired product and also conversion technique.

2.4.2 Preparation of heterogeneous catalyst

1) Impregnation: This technique is used to impregnate metal site on support surface. The chosen metal precursor is dissolved in solution that is the medium for impregnation process. Support material, which is solid, is immersed in the prepared precursor solution and then stirred for specific time depending on type of support and metal precursor. Sonication is sometimes used to assist metal to be impregnated on catalyst surface.

2) Incipient wetness impregnation: This technique is slightly similar to impregnation method but incipient wetness impregnation basically employs volume of precursor solution equal to total pore volume of support. Volume of precursor solution is the same as that of pore volume of support. Precursor solution is dropped onto the support catalyst and then capillary force assists impregnation process instead of diffusion which is comparably slow.

3) Precipitation: It introduces nucleation and growth processes for synthesis of catalyst. Adjustment of pH is involved. Base solution is added to the acid metal-containing solution in order to create the precipitation of metal onto the catalyst support, which is called forward precipitation. Reverse precipitation is the process where acid metal-containing solution is added to the base solution[20].

2.5 Literature review

2.5.1 Hydrothermal gasification of biomass and its model compounds

In order to find out the influence of molecular structures of biomass on its gasification performance, Castello, Kruse and Fiori [12] reported that phenol was extremely hard to gasify in comparison with glucose because mostly gaseous product was mainly produced from glucose after employing feedstock with organics content of 5 wt% by varying a relative concentration of phenol to glucose from 0-30 wt%. However, phenol preferred to react in liquid phase observed from reduction of phenol in terms of conversion. Moreover, glucose and phenol had no effect on each other because produced gas to glucose ratio remained constant despite change of their concentrations [12].

Safari et al. [18] employed three lignocellulosic materials consisting of wheat straw, walnut shell and almond shell in SCWG. Wheat straw which possessed the lowest amount of lignin gave the highest hydrogen and carbon gasification efficiencie which were 42.6 and 46.9 % respectively. It also produced the highest hydrogen gas yield equal to 6.52 mmol per gram of biomass whereas the others provided 4.26 and 4.1 mmol per gram of biomass for walnut shell and almond shell, respectively. They concluded that lignin content in biomass was an obstacle for gasification reaction which subsequently reduced gas production or gas yield because of its higher strength compare to cellulose and hemi-cellulose which were easier to be hydrolyzed and then gasified into gaseous product [18].

Chuntanapum and Matsumura [13] conducted 5-(Hydroxymethyl)furfural (5-HMF) to be gasified in sub- and supercritical water conditions with temperature of 350 and 450 °C, respectively, and pressure of 25 MPa. Furthermore, effects of residence time and initial 5-HMF concentration on tarry material formation were also examined. Initial 5-HMF concentration ranged from 0.02-0.15 M with residence time varying from 80-3000 s. 5-HMF strongly distributed to tar and char products especially in subcritical water with high concentration of 5-HMF. Gas yields obtained from gasification of all the initial 5-HMF concentrations were almost the same. Supercritical water gasification produces no char obviously in contrast with gasification under subcritical condition which can observe char in whole range of residence time employed in this work and found higher amounts of char in longer residence time [13].

Promdej and Matsumura [14] studied the effect of temperature on glucose decomposition under sub- and supercritical water. Temperature was in a range of 573-733 K, which covered sub- and supercritical regions. Char production could be highly inhibited under supercritical water. Gas production increased significantly with increase in temperature [14].

Susanti et al. [15] studied the gasification of oxygenated hydrocarbons. Methanol, ethanol, glucose and glycerol were easier to be gasified than the other feed stocks which were long chain hydrocarbons at 740 °C and concentration of 10 wt%. Carbon gasification efficiency (CGE) of over 90% was achieved in all feed stocks. Regard to the effect of temperature, CGE of 99% was succeeded when methanol was used as a feed stock in the experiment in which temperature was set at 650 °C while iso-octane and n-decane, which possess higher amount of carbon atom in their chain molecules, provided smaller CGE than methanol which was 80% and 78%, respectively. Raising the temperature to 750 °C, methanol, iso-octane and n-octane succeed in complete carbon gasification. When concentration of feed stocks increase to 20 wt%, the results showed that n-decane was easier to be gasified than iso-octane. It can be concluded that branch-chain molecule had more resistance to be gasified than linear-chain molecule of hydrocarbon [15].

Castello et al. [16] performed SCWG. Glucose and phenol representing model compounds of cellulose and phenol, respectively, were employed in SCWG. Four different glucose/phenol content mixtures were prepared ranging from pure glucose to phenol content of 30 wt% by maintaining the total organic content in water at 5 wt%. Phenol does not play a role in total gas production because gaseous products produced from all mixtures exhibit a quite similar amounts of gas produced per gram glucose although phenol seem to reduce hydrogen production as its content increase. Moreover, phenol favor de-hydration reaction but it suppress de-carbonyl reaction [16].

Watanabe et al. [17] studied the effect of heating rate on gasification of glucose. The heating rate of 4.2 K/s using sand bath without shaking gave a complete gasification of glucose at temperature of 623 K. A temperature increase led to higher gas yield which can be explained by enforcing a bond breaking reaction to form gaseous product at higher temperature instead of dehydration path way which could produce more furfural and phenol. The water-gas shift reaction and CO production from biomass conversion are favored when a temperature was increased. Rapid heating rate could provide more CO generation. At the temperature of 773 K, 20% of carbon contained in glucose could be converted when tin bath was used as a heating medium and subsequently providing very fast heating rate of 12.5 K/s [17].

2.5.2 Catalytic hydrothermal gasification of biomass and its model compounds

Zhang et al. [3] experimented on SCWG of glucose solution, by-product from hydrothermal liquefaction, and its model compounds consisting of glucose, acetic acid, and guaiacol. Continuous flow reactor was implemented for SCWG of their feedstock. RuNi/gamma-Al_2O_3 and RuNi/Activated carbon (AC) were employed to study their effects on SCWG. Ni content was 10 wt% and the molar ratio of Ru to Ni was 0.1 for both catalysts. Because real organic waste had alkali and nitrogen, RuNi/gamma-Al_2O_3 was affected by those compounds resulting in significant deterioration whereas AC showed higher stability against real organic waste gasification in supercritical water. SCWG of glucose at 700 ◦C provided 9.8 mol

H_2/kg dried feedstock and CGE was 93.6 %. Regarding effect of RuNi/gamma-Al_2O_3, increasing temperature from 600 to 750 ◦C resulted in increase in hydrogen yields from 25.5 to 53.9 mol/kg dried feedstock and also increase in CGE from 99.2 to 99.6 %. It can be noted that RuNi/gamma-Al_2O_3 had a strong effect on H_2 yield while it slightly affected CGE value. Furthermore, study of concentration of glucose in feedstock showed that increase in feedstock concentration could reduce hydrogen yield but increased char yield. Ru combined with Ni in this research suggested that they had strong effects on SCWG of organic substances[3].

Azadi et al. [21] conducted catalytic reforming of glucose, glycine, glycerol, lauric acid and humic acid, representing carbohydrates, proteins, alcohol, fatty acids and humic substances, respectively, in batch type reactor with supercritical water. Glucose and glycerol showed higher carbon gasification ratio (CGR) and total gas yield with additional raney nickel catalyst loading than the humic acids, glycine, and lauric acid. The compounds comprising higher amounts of C-C bonds resulted in lower conversion except for the glycine which has a nitrogen atom in its structure. Raney nickel provided a high efficiency toward gasification of organic material[21].

Osada et al. [22] reported that Ru and Ni catalyst enhanced catalytic gasification of lignin and cellulose with a ruthenium catalyst in supercritical water at low temperature as 400 °C. Cellulose and lignin were gasified slightly without catalyst. Ru showed the best quality toward catalytic gasification of biomass[22].

Kaya et al. [23] studied effect of various type of carbon-based materials as catalyst supported with platinum (Pt) as active site on reforming of lignocellulosic biomass hydrolysate. It was reported that SWCNT provided higher catalytic activity compared to multi walled-carbon nanotube (MWCNT) due to hindrance effect of several narrow grapheme sheets of MWCNT against accessibility of reactant onto inner MWCNT surface[23].

According to the above literature reviews, it can be concluded that the undesired products produced from glucose can undergo polymerization to generate char product and subsequently reduce yield of gaseous product. The efficient catalyst

used for enhancing gasification process is nickel and ruthenium. This kind of metals leads to an increase in gas production, especially hydrogen gas via water-gas shifted reaction.

Nickel has been proved to be efficient toward gasification reaction and also water-gas shift reaction. Thus, gas yield and hydrogen content can increase. Ruthenium also had advantages against gasification of biomass feedstock and model compounds as it enhances hydrogen, methane productions, and conversion of biomass. However, few researchers have studied co-existing of Ni and Ru on supporting catalyst, especially carbon-based catalysts. Furthermore, SWCNT possesses appropriate physical and chemical properties which are suitable for being used as catalyst support. Hence, SWCNT was introduced with Ni and Ru as active sites to study their effects on SCWG of glucose.

CHAPTER III

EXPERIMENTAL

Catalyst synthesis preparation is composed of functionalization of SWCNT with acid solution to partially activate surface of SWCNT and, consequently, changing its morphology. Then, oxygenated functional groups were added on SWCNT surface, named functionalized SWCNT (FSWCNT), which can subsequently react with metal precursors and receive anchoring of metals onto SWCNT surface. Metals employed in this research consist of Ni and Ru which come from different types of precursors. Ni/SWCNT and Ru-Ni/SWCNT are synthesized via impregnation, calcination, and lastly reduction with hydrogen gas to activate metal active sites.

3.1 Materials

1) Single walled carbon nanotube (Purity of carbon > 90%), Diameter 2 nm(±0.5)
2) Sulfuric acid 97%
3) Nitric acid 60%
4) $Ni(CH_3COO)_2 \cdot 4H_2O$ 98%
5) $RuCl_3 \cdot XH_2O$ (Ru content = 40-49%)
6) DI water
7) Ethanol 96%
8) Glucose 98%

3.2 Characterizing instruments

1) Gas chromatography (GC-14B) from Shimadzu, connected with thermal conductivity detector (TCD) and flame ionization detector (FID), was used to determine gas product composition produced from hydrothermal gasification of glucose experiments.

2) Total organic carbon analyzer (TOV-V CPH) from Shimadzu was used to determine TOC dissolved in liquid products obtained from hydrothermal gasification of glucose experiments and also inorganic carbon (IC) resulting from dissolvation of some gas product in liquid phase.

3) High-performance liquid chromatography (HPLC) was used to determine quantity of some chemicals in liquid product

4) Energy-dispersive X-ray spectroscopy (EDX) was used to confirm an existing of metal impregnated on carbon nanotube

5) X-ray diffraction (XRD-D8 Advance) from Bruker was used to determine Ni/SWCNT and Ru-Ni/SWCNT for analysis of metal phase on tube surface, after calcination and reduction.

6) Transmission electron microscopy (TEM) was used to qualitatively determine morphology of Ni/SWCNT and Ru-Ni/SWCNT, after impregnation and calcination.

3.3 Functionalization of SWCNT

1) Firstly, 70 ml of acidic mixture was prepared by mixing 35 ml of 8 M sulfuric solution and 35 ml of 8 M nitric solution, which are prepared by diluting concentrated acid solution of each type with deionized water.

2) SWCNT with an amount of 3 g was immersed in 70 ml sulfuric/nitric solution in the flask and stirred using magnetic stirrer for 15 min.

Temperature of the mixture was adjusted manually at 60 ◦C. Speed of magnetic stirrer was set constantly at 700 rpm.

3) After stirring process, the magnetic stirrer was separated from the resulting mixture. The flask containing the mixture was then placed in the ultra-sonicator for 2 h in order to assist acidic functional group to be anchored on the SWCNT.

4) Dilution process of the mixture was essential to stop the functionalization process. For this purpose, the resulting mixture after sonication was diluted with DI water until the total volume of 500 ml was achieved. Magnetic stirrer was employed to shorten the dilution time. DI water was always analyzed with pH meter in order to reach the final point of this process. In other word, the final pH of the mixture should be equal to that of DI water which was 5.

5) Filtration process was done by using the filter paper made of cellulose fiber. The pH value of water was measured with pH meter which was around 5. The pH meter was always validated by measuring the solutions whose pH values were known. If the pH value shown in monitor was similar to that of the pH value of the indicator solution, it can be used instantly. But, if the pH value had an error, tuning had to be done prior to the experiment.

3.4 Impregnation

1) Nickel (II) acetate tetra hydrate ($Ni(CH_2COO)_2 \bullet 4H_2O$) was chosen as Ni precursor for producing Ni/SWCNT via impregnation method. Ruthenium (III) chloride hydrate ($RuCl_3 \bullet XH_2O$) was used as Ru precursor as well. Impregnation medium was the mixture of 2 ml of ethanol and 18 ml of DI water. Hence, the total volume of impregnation medium was 20 ml.

2) Firstly, the mixture of metal precursor and impregnation medium was prepared. Only $Ni(CH_2COO)_2.4H_2O$ was added in case of synthesizing Ni/SWCNT whereas both $Ni(CH_2COO)_2.4H_2O$ and $RuCl_3.XH_2O$ were used in case of synthesizing Ru-Ni/SWCNT. The chosen contents of Ni and Ru are 16.7 wt% and 5 wt% of the total weight of catalyst, respectively. Regarding Ni/SWCNT, 0.0865 g of $Ni(CH_2COO)_2.4H_2O$ was added into impregnation medium solution. In case of Ru-Ni/SWCNT, 0.0922 g of $Ni(CH_2COO)_2.4H_2O$ and 0.0146 g of $RuCl_3.XH_2O$ were both added. After that, 0.1 g of FSWCNT was immersed in the mixture of precursor and stirred magnetically at room temperature for 48 h. Then, it was filtered using filter paper and washed with DI water several times before dried in an oven overnight at 80 ◦C.

3.5 Calcination and reduction

Catalysts after impregnation method were calcined and reduced, respectively. Calcination process has been done at temperature of 400 °C. Catalyst was exposed to a flow of nitrogen gas for 3 hours. Afterward, reduction process has been done at the same condition by using a flow of hydrogen gas instead before cooling down with a flow of nitrogen gas. Flow rate of each gas was set at 40 ml/min. Finally, reduced catalysts were carefully collected in plastic bags being full of nitrogen gas.

3.6 Supercritical water gasification of glucose

Gasification apparatus (as shown in Fig. 3.1) consisted of furnace, batch-type reactor made from stainless steel 316 with inner diameter of 7.4 mm, salt bath, 2 thermocouples which were used to measure temperature in salt bath and reactor, ball valve, and gas sampling port. Electricity generator was used for manually adjusting the temperature of salt bath. Temperature logger was used as temperature monitoring 2 positions as shown in Fig. 3.1. After the temperature of salt bath was 400 ◦C, the stainless steel tube reactor, which was already filled with the desired amount of

reactant solution and/or catalysts including SWCNT, FSWCNT, Ni/SWCNT, and Ru-Ni/SWCNT, is immersed in the salt bath for various reaction time (15-60 min).

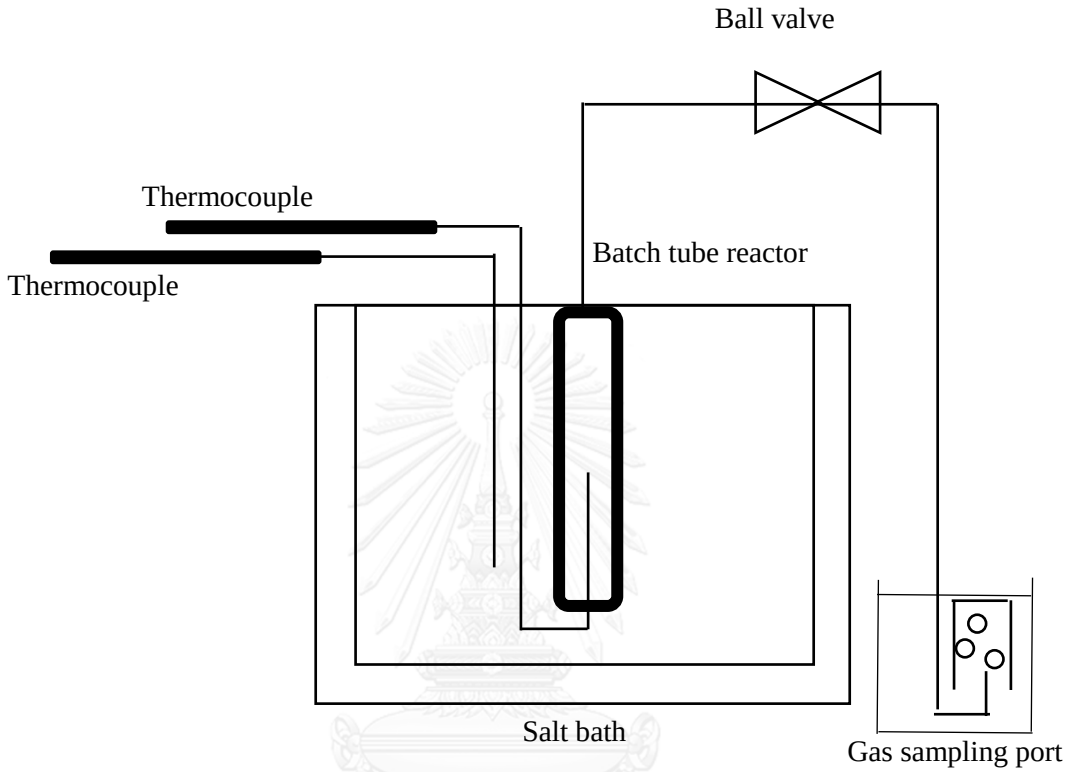

Fig. 3.1 Schematic diagram of gasification apparatus

All product yields were calculated based on carbon atom as shown below.

$$\text{product yield } [-] = \frac{\text{carbon content in product [mol C]}}{\text{carbon content in feedstock [mol C]}} \qquad (3.1)$$

So that, gas yield was carbon gasification efficiency (CGE). Liquid yield was total organic carbon (TOC) yield, and solid yield was char yield.

3.7 Calculation of pressure in the batch-type reactor

Specific volume = $\hat{V}$

Reactor volume = V

Mass of water = m

Mass of water required for reaction pressure to reach 25 MPa at temperature of 400 ◦C can be calculated from the following equation.

$$\hat{V} = \frac{V}{m} \qquad (3.2)$$

From Fig. 3.2, at temperature of 400 ◦C and pressure of 25 MPa, specific volume of water is 0.0060047 m^3/kg. The volume of reactor is 0.0000076 m^3. So that, the mass of water required is 1.226 g. If density of water is 1 g/cm^3, volume of water required is 1.226 cm^3. In this research, 1.38 cm^3 of 5 wt% glucose solution was used as feedstock. The density of feedstock is 1.019 g/cm^3, determined by weighing the glucose solution with an exact volume, so that the volume of water truly added into the reactor can be calculated and was 1.33 cm^3 which can ensure the supercritical water condition.

Table 3.1 Compressed water and superheated steam

25 MPa					30 MPa					35 MPa			
v	*ρ*	*h*	*s*	*t*, ℃	*v*	*ρ*	*h*	*s*	*t*, ℃	*v*	*ρ*	*h*	*s*
1.3459	743.02	1331.3	3.1919	**300**	1.3322	750.66	1328.9	3.1760	**300**	1.3197	757.74	1327.0	3.1612
1.3810	724.09	1384.1	3.2832	**310**	1.3646	732.80	1380.4	3.2652	**310**	1.3499	740.78	1377.6	3.2486
1.4215	703.49	1438.9	3.3764	**320**	1.4014	713.58	1433.7	3.3557	**320**	1.3837	722.67	1429.5	3.3370
1.4690	680.74	1496.4	3.4726	**330**	1.4436	692.69	1489.1	3.4483	**330**	1.4220	703.22	1483.2	3.4268
1.5264	655.13	1557.5	3.5731	**340**	1.4932	669.70	1547.1	3.5438	**340**	1.4660	682.13	1539.1	3.5186
1.5988	625.45	1623.9	3.6804	**350**	1.5529	643.95	1608.8	3.6436	**350**	1.5174	659.01	1597.6	3.6132
1.6969	589.31	1698.6	3.7993	**360**	1.6276	614.39	1675.6	3.7498	**360**	1.5791	633.29	1659.6	3.7120
1.8503	540.46	1789.8	3.9423	**370**	1.7268	579.09	1750.1	3.8666	**370**	1.6554	604.08	1726.5	3.8168
2.2182	450.82	1935.7	4.1671	**380**	1.8729	533.93	1838.2	4.0025	**380**	1.7546	569.94	1800.4	3.9308
4.6474	215.18	2395.7	4.8660	**390**	2.1331	468.81	1955.3	4.1804	**390**	1.8930	528.27	1885.4	4.0599
6.0047	166.54	2578.6	5.1400	**400**	2.7978	357.43	2152.8	4.4757	**400**	2.1054	474.97	1988.6	4.2143
6.8833	145.28	2687.1	5.3000	**410**	3.9809	251.20	2395.4	4.8336	**410**	2.4747	404.09	2123.9	4.4138
7.5792	131.94	2769.4	5.4197	**420**	4.9203	203.24	2552.9	5.0627	**420**	3.0838	324.28	2291.9	4.6579
8.1725	122.36	2837.8	5.5176	**430**	5.6366	177.41	2662.8	5.2200	**430**	3.7800	264.55	2447.6	4.8809
8.6986	114.96	2897.3	5.6016	**440**	6.2267	160.60	2748.9	5.3416	**440**	4.4120	226.65	2571.8	5.0564

CHAPTER IV

RESULTS AND DISCUSSION

4.1 Catalyst characterization

In this part, catalyst characterization was described in terms of several kind of parameters including surface area, pore volume, pore diameter, morphology, elemental confirmation, and form of metal on catalysts.

4.1.1 SEM-EDX

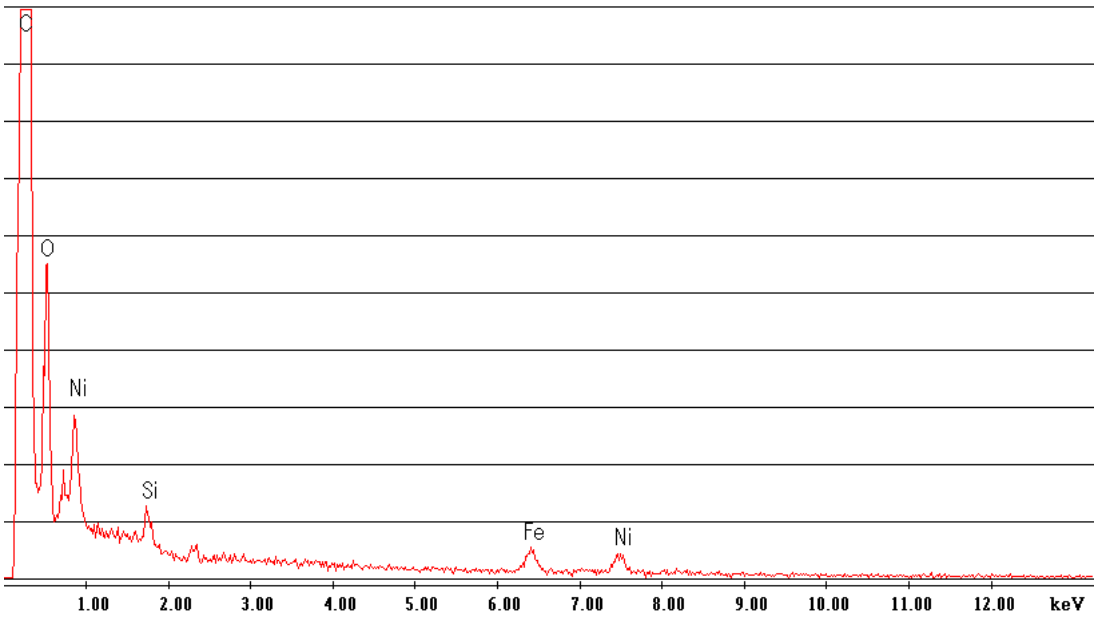

Fig. 4.1 EDX spectrum pattern of Nickel Acetate-impregnated SWCNT

At first step before calcination and reduction process, SEM-EDX analysis was employed to give confirmation of elemental species with easy sample preparation step unlike TEM or XRD. So, SEM-EDX analysis was employed as shown in **Fig. 4.1-4.2**. Fig. 4.1 demonstrated EDX spectrum pattern of Nickel Acetate-impregnated SWCNT which exhibited several elements consisting of C, O, Ni, Si, and Fe. C and O can be

attributed to the carbon nanotubes and acid treatment process because this sample had not been processed at high temperature in calcination process but only underwent drying process at 100 °C in natural convection oven. Trace amount of Fe can be observed as the impurity from the manufacturer of the SWCNT used in this study which decreased after acid treatment.

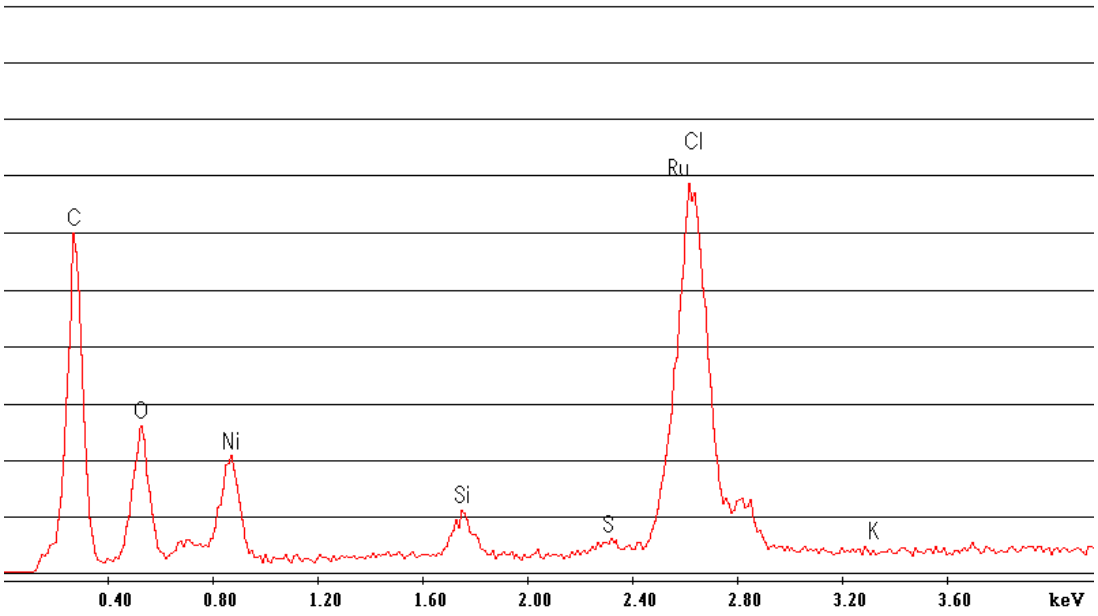

Fig. 4.2 EDX spectrum pattern of Ruthenium Chrolide-impregnated SWCNT

Fig. 4.2 indicated an existence of C, O, Ni, Ru, Cl, and the other trace amount of impurity. C peak comes from carbon nanotubes while O peak is attributed to functional groups resulting from functionalization process with acidic solution. Ru and Cl peaks were found according to ruthenium (III) chloride as Ru precursor which came from impregnation step.

4.1.2 BET analysis

N_2 adsorption analysis was conducted on SWCNT, FSWCNT, Ni/SWCNT, and Ru-Ni/SWCNT to determine BET surface area, total pore volume, and mean pore diameter. The results were shown in **Table 4.1**. After SWCNT was treated with acid solution, BET surface area increased, possibly due to demolishing of a bundle of tubes [24]. Hence, a bundle of tubes could undergo disentanglement and becomes more individual. BET surface area of SWCNT was 444 m^2/g while that of functionalized-single-walled carbon nanotube (FSWCT) increased to 848 m^2/g. These values can be confirmed by Prigney et al. [25] who formulated the correlation between a number of wall layer, an amount of tubes in a bundle, diameter, and specific surface area, which gives a good agreement with the experimental data [25]. They reported that one individual SWCNT possesses 1,315 m^2/g and becomes less to 751, 484, 151 m^2/g when a bundle of tubes grows larger from 7 to 19 and 217 tubes, respectively. As a result, hidden pores could be exposed to the environment which is mostly composed of a number of smaller pores compared to as-received SWCNT and mean pore diameter of FSWCT then decreased. Once FSWCNT was impregnated with nickel and underwent calcination process at 400 °C under nitrogen flow, BET surface area increased from 848.64 to 1,382.30 m^2/g. This result suggested that nickel catalyst didn't cause pore blockage but increased surface roughness of the tubes and also introduced pores to the whole support, instead. However, after both nickel and ruthenium were impregnated onto carbon nanotubes, surface area became 1,159.60 m^2/g which is higher than FSWCNT but lower than Ni/SWCNT. It may appear that both metals can increase surface roughness and provide pores to the catalyst leading to an increase in surface area of Ni/SWCNT and Ru-Ni/SWCNT. However, introducing ruthenium together with nickel resulted in increase in degree of agglomeration and pore blockage which reduced surface area, suggesting that higher metal loading leads to less surface area.

Considering total pore volume, it was observed that acid treatment can disassemble a bundle of SWCNT leading to hidden pore opening and then significantly increasing total pore volume from 0.6991 to 0.9436 cm^3/g. Total pore volume continue to increase from 0.9436 to 1.0657 cm^3/g when nickel appears on tube surface. Further increasing metal loading by adding nickel and ruthenium to the carbon nanotubes led to an agglomeration, pore blockage as mentioned earlier and consequently reducing total pore volume from 1.0657 to 0.9097 cm^3/g. This result is identical to recent literature[2].

Mean pore diameter decrease from 6.2929 to 4.4478 and 3.0839 nm after acid treatment and nickel impregnation, respectively. It was because acid treatment can cause pore opening. Metal supported on carbon nanotube itself also possesses many small pores which have been taken into analysis.

Table 4.1 BET analysis

	SWCNT	**FSWCNT**	**Ni/SWCNT**	**Ru-Ni/SWCNT**
BET surface area (m^2/g)	444.35	848.64	1,382.30	1,159
Total pore volume (cm^3/g)	0.6991	0.9436	1.0657	0.90
Mean pore diameter (nm)	6.2929	4.4478	3.0839	3.1

4.1.3 XRD

XRD was introduced in order to investigate the effect of acid treatment, calcination, and reduction processes against structure of carbon nanotubes and metals on their surface.

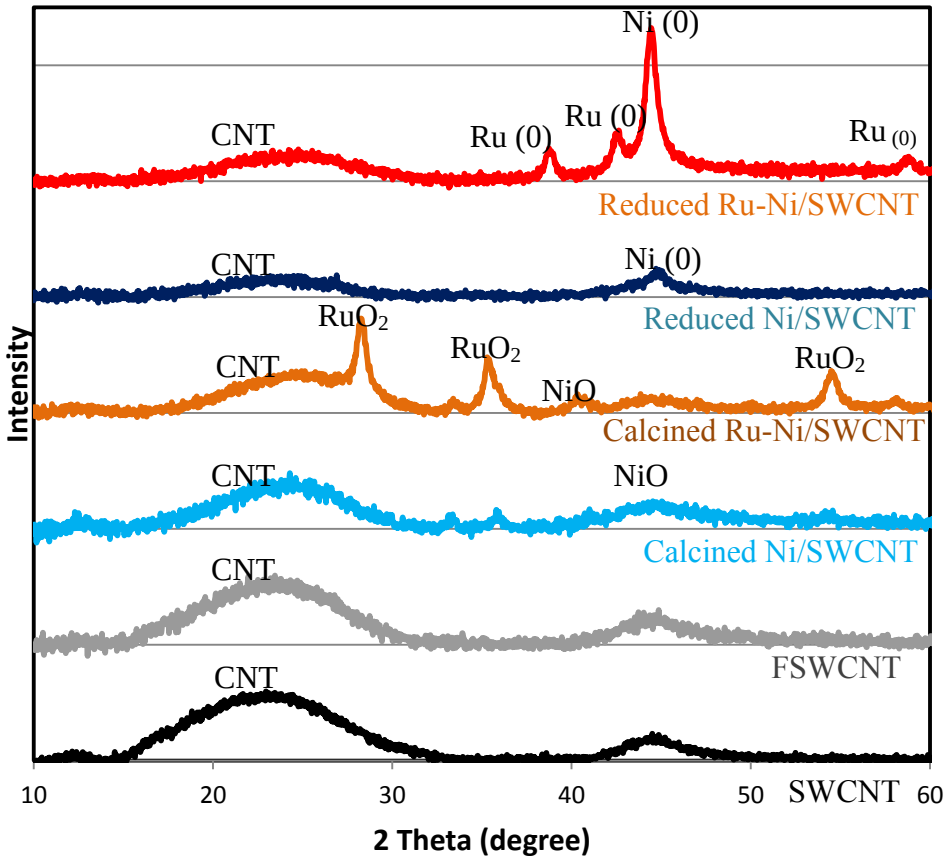

Fig. 4.3 XRD patterns of SWCNT, FSWCNT, calcined and reduced catalysts

It seems that acid treatment caused no change of structure and crystallinity of tubes according to XRD patterns of SWCNT and FSWCNT as shown in **Fig. 4.3**. They gave almost identical peak at $2\theta=26^{o}$ which represents graphitic carbon nanotube diffraction, suggesting that acid treatment did not lessen crystalline structure of carbon nanotube. Calcined Ni/SWCNT showed XRD peak at $2\theta=43.3^{o}$ which is attributed to NiO while reduced Ni/SWCNT exhibited peak of Ni (0) at $2\theta=44.6^{o}$.

Regarding calcined Ru-Ni/SWCNT, peaks located at $2\theta= 28.1^{o}$, 35.1^{o}, and 54.4^{o} confirmed an existence of RuO_2 on carbon nanotubes associated with peak at $2\theta=43.3^{o}$ of NiO. According to reduced catalysts, it can be observed that there were peaks at $2\theta=38.4^{o}$, 42.2^{o}, and 58.2^{o} representing Ru (0) and peak at $2\theta=44.6^{o}$ owned by Ni (0). It can be concluded that calcination process and reduction processes were successfully done under temperature of 400 °C.

4.1.4 TEM

TEM analysis was conducted to study effect of catalyst synthesis steps on particle size and particle size distribution of metal on SWCNT.

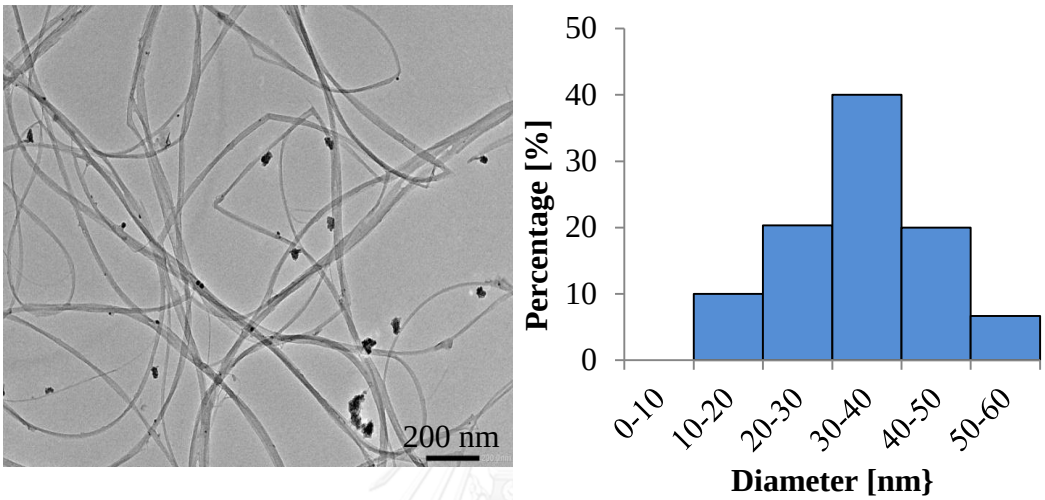

Fig. 4.4 a) TEM images and b) particle size distribution of Ni/SWCNT after impregnation

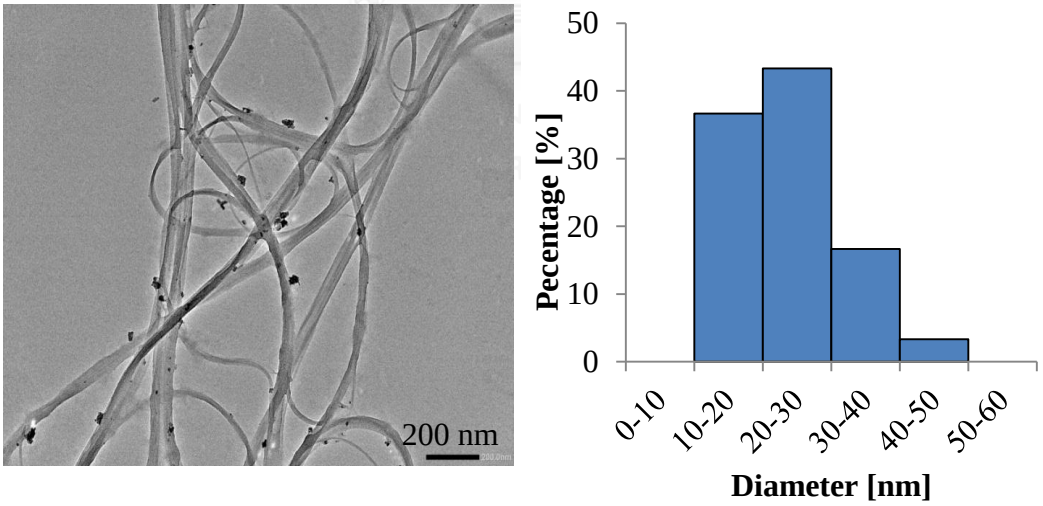

Fig. 4.5 a) TEM images and b) particle size distribution of Ni/SWCNT after calcination

Fig. 4.4-4.5 demonstrated TEM images of Ni/SWCNT before and after calcination process, respectively. Sizes of metal particles embedded on carbon nanotubes were constant between Ni/SWCNT before and after calcination process.

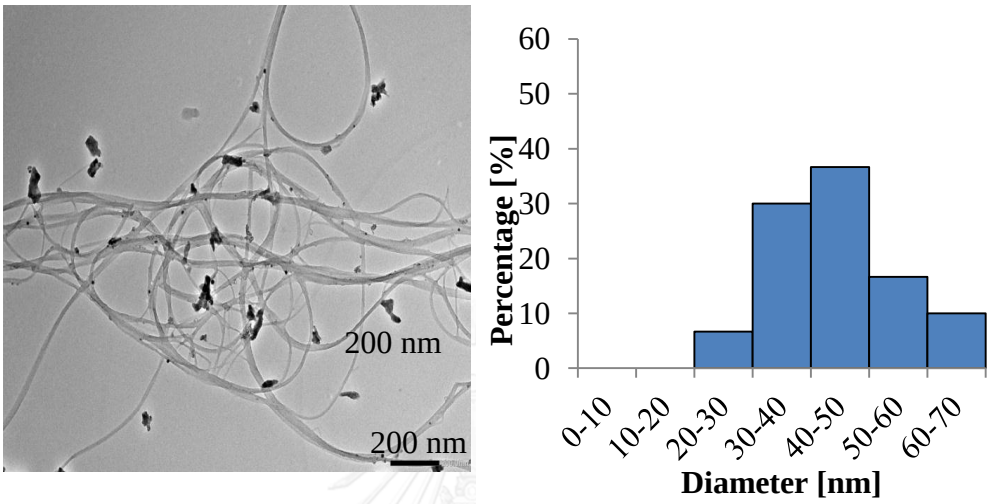

Fig. 4.6 a) TEM images and b) particle size distribution Ru-Ni/SWCNT after impregnation

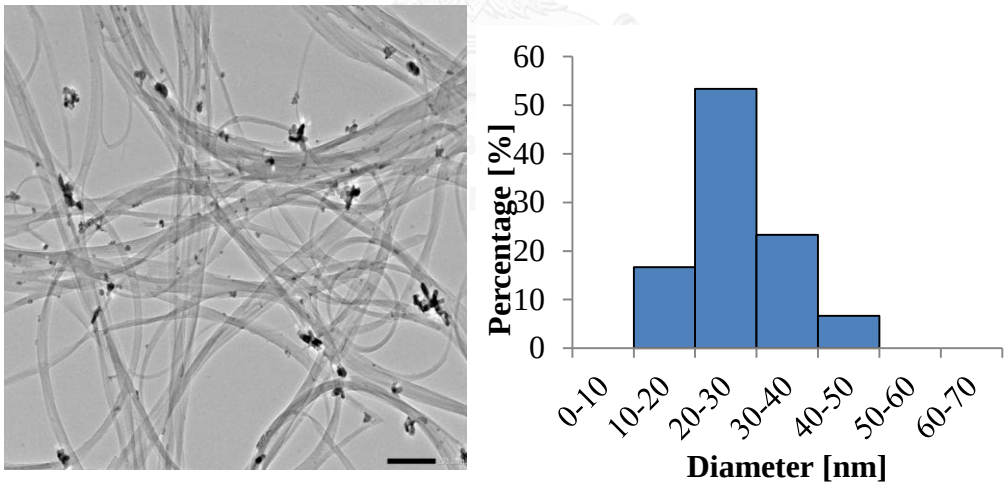

Fig. 4.7 a) TEM images and b) particle size distribution of Ru-Ni/SWCNT after calcination

TEM images of Ru-Ni/SWCNT after impregnation and Ru-Ni/SWCNT after calcination were shown in **Fig. 4.6-4.7**, respectively. It can be seen that the particle size seemed to reduce after calcination step with high temperature.

4.2 SCWG of glucose with various reaction time

Effect of reaction time on gasification product of glucose was studied in terms of gas product composition, CGE yield, TOC yield, char yield, and gas yield.

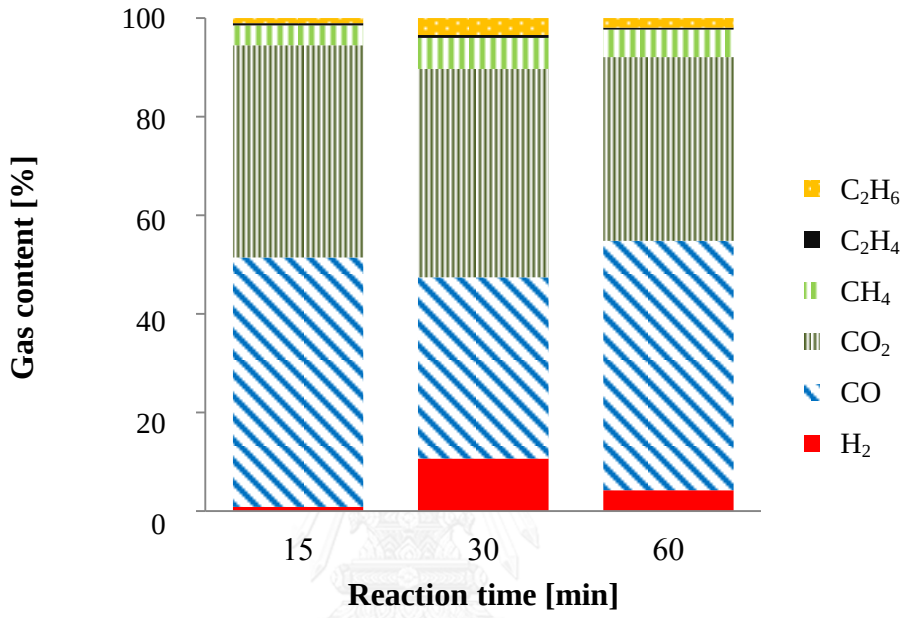

Fig. 4.8 Effect of reaction time on gas product composition from SCWG of glucose without catalyst at temperature of 400 °C and pressure of 25 MPa

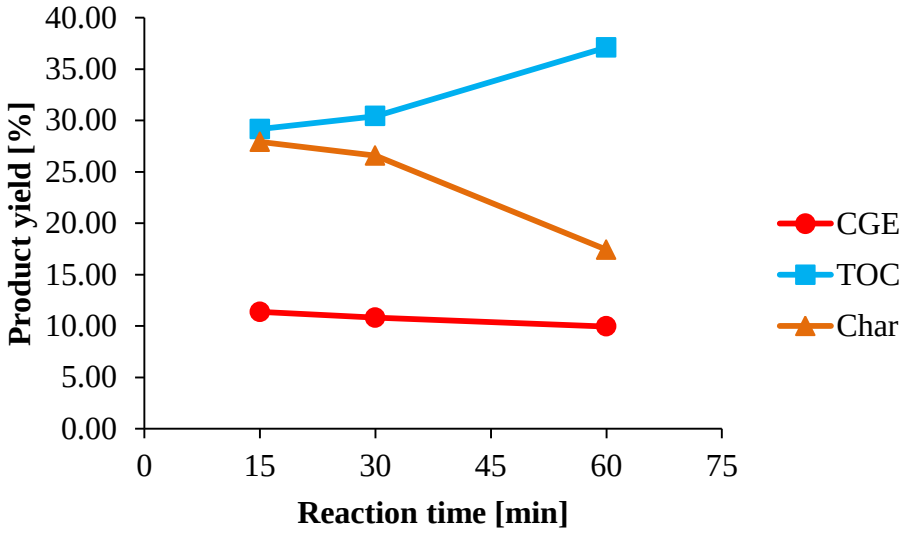

Fig. 4.9 Effect of reaction time on CGE, TOC, and char yields from SCWG of glucose without catalyst at temperature of 400 °C and pressure of 25 MPa

From **Fig. 4.8**, considering gas product composition, it can be observed that hydrogen was produced the most at 30 min. When reaction time was lengthened from 30 to 60 min, amount of hydrogen decreased significantly on the average from 10.65 to 4.22 vol% along with a slight decrease in amount of carbon dioxide on the average from 42.22 to 37.24 vol%. On the other hand, amount carbon monoxide increased roughly from 36.77 to 50.60 vol%. Hence, it can be concluded that water-gas shift reaction was favorable at 30 min of reaction time and an increase in reaction time to 60 min led to a decrease in hydrogen content.

From **Fig. 4.9,** CGE is in a range of 9.52-13.78 %. It can be implied that reaction time does not affect CGE obtained from SCWG of glucose at 400 °C and 25 MPa with various reaction time in a range of 15-60 min. However, TOC yield increased whereas char yield decreased with reaction time.

Table 4.2 Effect of reaction time on gas yields from SCWG of glucose (No catalyst) at temperature of 400 °C and pressure of 25 MPa

Reaction time [min]	**Gas yield [mmol/g glucose]**						
	CO	**CO_2**	**CH_4**	**C_2H_4**	**C_2H_6**	**H_2**	**Total gas**
15	1.882	1.577	0.149	0.017	0.049	0.027	3.701
30	1.418	1.608	0.244	0.021	0.135	0.399	3.823
60	1.685	1.229	0.181	0.015	0.062	0.143	3.315

Considering each gas yield as shown in **Table 4.2**, the highest total gas yield of 3.823 mmol/ g glucose can be obtained at reaction time of 30 min. Furthermore, hydrogen yield increased from 0.027 to 0.399 mmol/g glucose after reaction time increased from 15 to 30 min. Surprisingly, extending reaction time from 30 to 60 min resulted in significant reduction of hydrogen yield from 0.399 to 0.143 mmol/g glucose. Moreover, CH_4 yield also increased to the highest yield at 30 min and decreased when reaction time was lengthened to 60 min. C_2H_6 yield also showed the same trend as that of H_2 and CH_4 yields. It can be implied that several different reaction pathways took place competitively in SCWG of glucose. From these results obtained from SCWG of glucose without catalyst, reaction time of 30 min is the most efficient condition in terms of hydrogen yield, methane yield, and total gas

production. Other gas yields showed no significant trends to be observed with reaction time increase.

4.3 SCWG of glucose on single walled-carbon nanotube

In order to investigate the effect of Ni and Ru metals as promising catalysts in SCWG of glucose in this study, effect of supporting material was firstly examined.

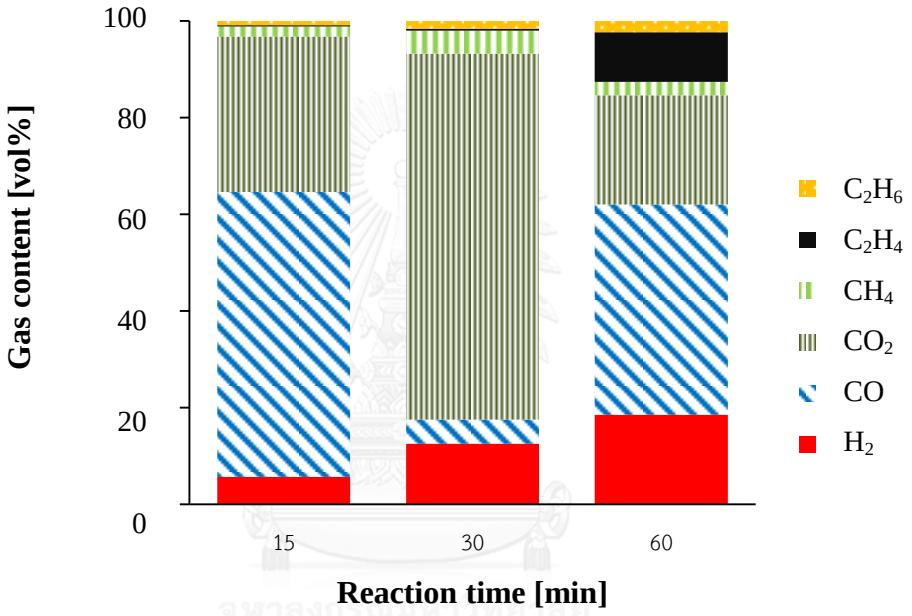

Fig. 4.10 Effect of reaction time on gas product composition from SWCNT-catalyzed SCWG of glucose at temperature of 400 °C and pressure of 25 MPa

It was shown in **Fig. 4.10** that H_2 content increases from 5.70 to 18.55 vol% with reaction time. Moreover, significant change in other products can be observed. Dramatic change of CO and CO_2 were observed with an increase in reaction time.

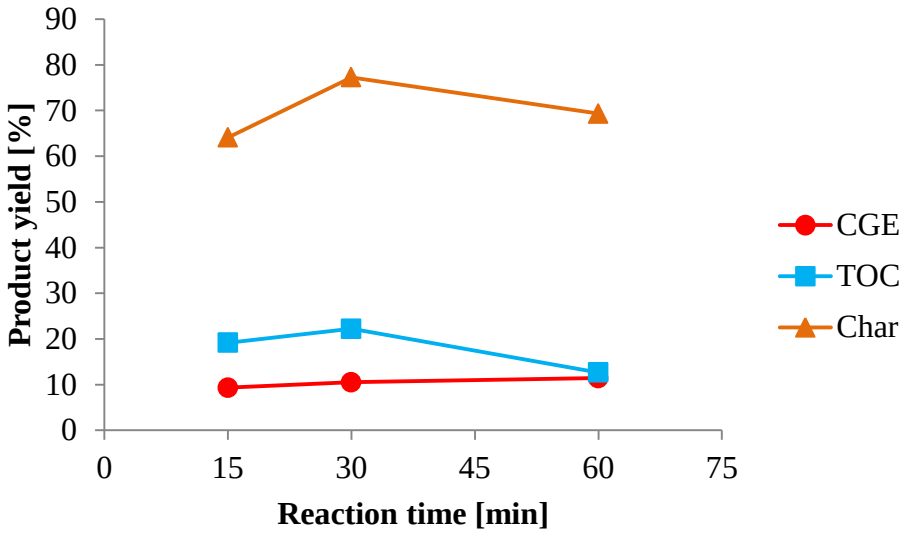

Fig. 4.11 Effect of reaction time on CGE, TOC, and char yields from SWCNT-catalyzed SCWG of glucose at temperature of 400 °C and pressure of 25 MPa

Fig. 4.11 shows that change of CGE can be considered negligible as it slightly increased from 9.33 to 11.44 when reaction time increased. TOC yield slightly increased from 19.19 to 22.21 % before significantly decreased to 12.66 % at 30 and 60 min, respectively. Char yield firstly increased from 64.11 to 77.28 % and then reduced to 69.31 vol%. It can be noted that some liquid products were gasified and polymerized into gaseous and char products, respectively, because of dramatic reduction of TOC yield when reaction time increased from 30 to 60 min.

Table 4.3 Effect of reaction time on gas yields from SWCNT-catalyzed SCWG of glucose at temperature of 400 °C and pressure of 25 MPa

Reaction time [min]	Gas yield [mmol/g glucose]						
	CO	**CO_2**	**CH_4**	**C_2H_4**	**C_2H_6**	**H_2**	**Total gas**
15	1.894	1.035	0.067	0.008	0.028	0.183	3.216
30	0.193	2.919	0.185	0.017	0.060	0.485	3.859
60	1.742	0.906	0.111	0.411	0.093	0.743	4.006

From **Table 4.3,** it can be observed that hydrogen and methane yields firstly increased whereas CO decreased significantly, suggesting that water-gas shift reaction and methanation, shown in equation 4.1, 4.2, and 4.3, were taking place at the first period of reaction time [17]. Also, carbon dioxide dramatically increased at first step

which supposedly produced via those gas phase reactions. However, after reaction time increased from 30 to 60 min, CO drastically increased which is possibly due to TOC consumption and reverse methanation reaction where CH_4 and CO_2 were consumed [26] as shown in Table 4.3.

$$CO + H_2O \rightleftharpoons H_2 + CO_2 \quad (4.1)$$

$$CO + 3H_2 \rightleftharpoons CH_4 + H_2O \quad (4.2)$$

$$CO_2 + 4H_2 \rightleftharpoons CH_4 + 2H_2O \quad (4.3)$$

4.4 SCWG of glucose on nickel supported single-walled carbon nanotube

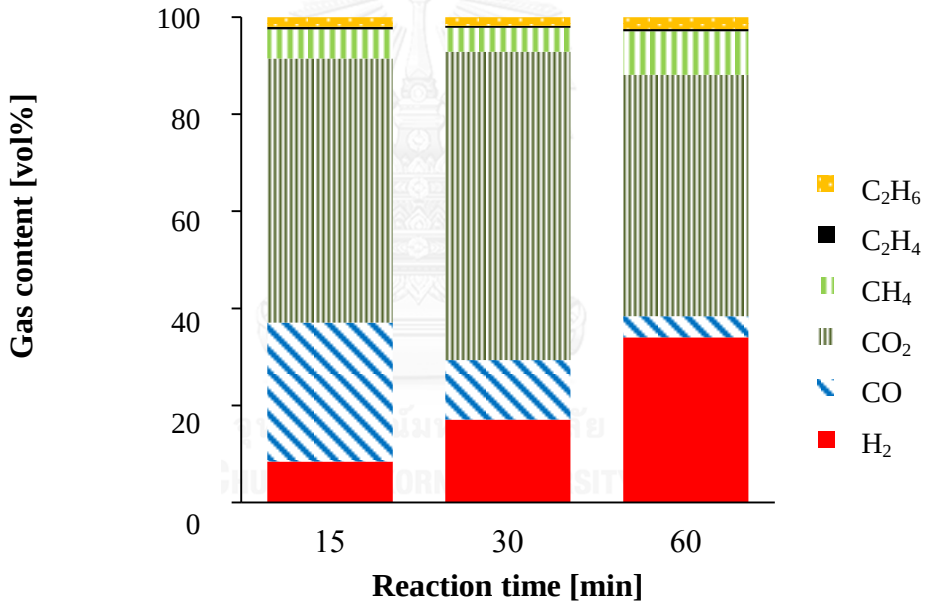

Fig. 4.12 Effect of reaction time on gas product composition from Ni/SWCNT-catalyzed SCWG of glucose at temperature of 400 °C and pressure of 25 MPa

According to Ni/SWCNT-catalyzed SCWG of glucose at 400 °C and 25 MPa with various reaction times in a range of 15-60 min. It can be seen from **Fig. 4.12** that hydrogen and methane contents considerably increased while carbon monoxide decreased with reaction time increase, implying that methanation and water-gas shift reaction competitively took place which consumed carbon monoxide. However, from **Fig. 4.13**, CGE increased from 13.00 to 16.51 % with an increase in reaction time

while TOC firstly increased from 13.65 to 25.29 % before decreased to 11.66 %, suggesting some intermediates in liquid phase were rapidly generated at the first period of reaction time and finally consumed into gas and char products. It can be concluded that some species in liquid phase were polymerized which resulted in an increase in solid production. According to this, there have been some studies reporting that 5-(hydroxymethyl)furfural (5-HMF) and furfural are responsible for char and tar production[13, 14]. Moreover, some other TOC can transform into gaseous product resulting in an increase in CGE.

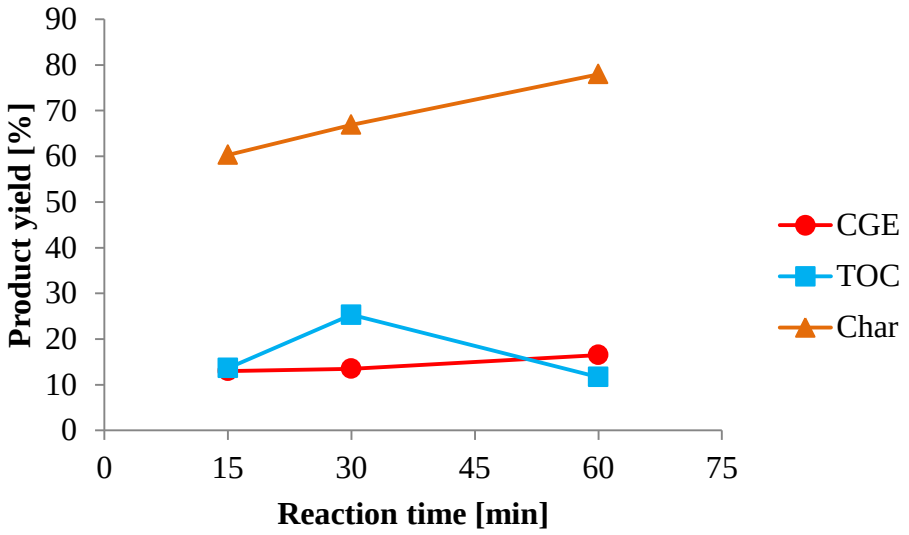

Fig. 4.13 Effect of reaction time on CGE, TOC, and char yields from Ni/SWCNT-catalyzed SCWG of glucose at temperature of 400 °C and pressure of 25 MPa

Table 4.4 Effect of reaction time on gas yields from Ni/SWCNT-catalyzed SCWG of glucose at temperature of 400 °C and pressure of 25 MPa

Reaction time [min]	Gas yield [mmol/g glucose]						
	CO	CO_2	CH_4	C_2H_4	C_2H_6	H_2	Total gas
15	1.306	2.488	0.273	0.024	0.091	0.388	4.569
30	0.635	3.287	0.254	0.022	0.093	0.885	5.175
60	0.347	3.957	0.713	0.032	0.197	2.706	7.952

From **Table 4.4**, it can be noted that an increase in reaction time from 15 to 60 min resulting in significant augmentation of methane and hydrogen yields. H_2 yield

increased significantly compared to other gases from 0.388 to 2.706 mmol/g glucose. It can be concluded that nickel catalyst influences production of methane and hydrogen via methanation and water gas-shift reactions. This can be confirmed by a decrease in CO consumed in those reactions which resulted in an increase in CO_2 as by-product.

4.5 SCWG of glucose on ruthenium and nickel supported single-walled carbon nanotube

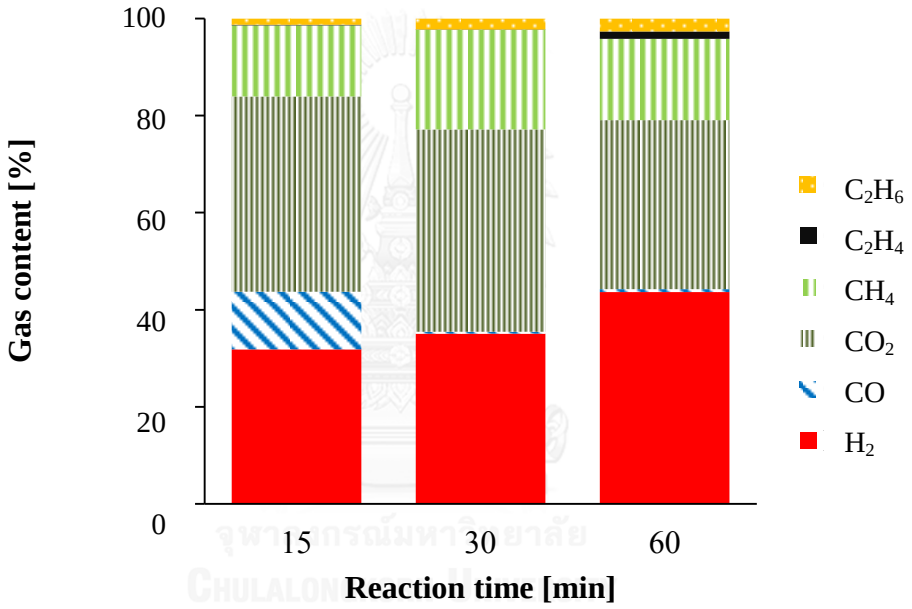

Fig. 4.14 Effect of reaction time on gas production from Ru-Ni/SWCNT-catalyzed SCWG of glucose at temperature of 400 °C and pressure of 25 MPa

In this part, effect of RuNi/SWCNT was investigated with reaction time increase in a range of 15-60 min. From **Fig. 4.14**, H_2 and CO_2 are the most abundant components in gaseous product for all reaction time, while CO strongly decreased from 11.89 to 0.43 vol% when reaction time increased from 15 to 30 min. It could be supposed that water-gas shift reaction, where CO, H_2, and CO_2 play an important role, took place in the reaction period.

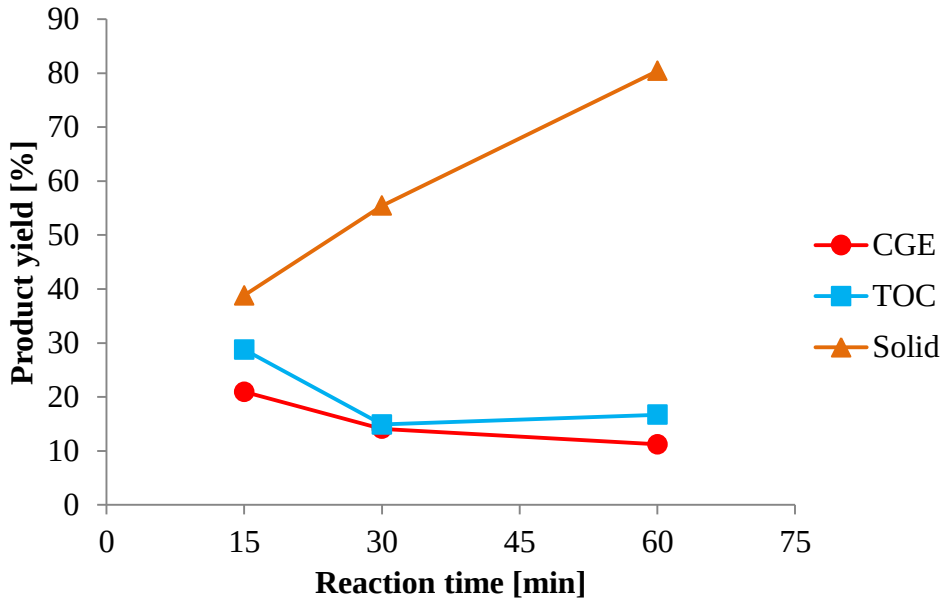

Fig. 4.15 Effect of reaction time on CGE, TOC and char yields from Ru-Ni/SWCNT-catalyzed SCWG of glucose at temperature of 400 °C and pressure of 25 MPa

Table 4.5 Effect of reaction time on gas yields from RuNi/SWCNT-catalyzed SCWG of glucose at temperature of 400 °C and pressure of 25 MPa

Reaction time [min]	**Gas yield [mmol/g glucose]**						
	CO	**CO_2**	**CH_4**	**C_2H_4**	**C_2H_6**	**H_2**	**Total gas**
15	1.158	3.919	1.421	0.013	0.123	3.099	9.733
30	0.030	2.883	1.423	0.002	0.154	2.428	6.920
60	0.035	2.073	0.995	0.094	0.155	2.602	5.954

But when considering yields of each product phase including gas, liquid and solid products as CGE, TOC and solid yields as shown in **Fig. 4.15**. TOC and CGE yield tend to decrease with reaction time increase. TOC yield decreased from 28.76 to 16.70 % and CGE yield also decreased from 20.94 to 11.23 %. Solid yield showed the different trend as it increased drastically from 38.81 to 80.40 %. As a result, TOC and gas yield possibly reacted with each other and, hence, produced solid product.

Table 4.5 showed that CO, CO_2, CH_4, and H_2 yield seemed to decrease with reaction time increase which resulted from an decrease in CGE and total gas yield.

4.6 Kinetic parameter determination

According to previous literatures explaining about reaction pathways of gasification of glucose in supercritical water [13, 14] as schematically shown in **Fig. 4.16**, the reaction rate constants have been determined with first order reaction as assumption for all reactions. It can be seen that glucose, fructose, furfural, and 5-HMF seems to be the key intermediates in liquid phase contributing to gas and char production.

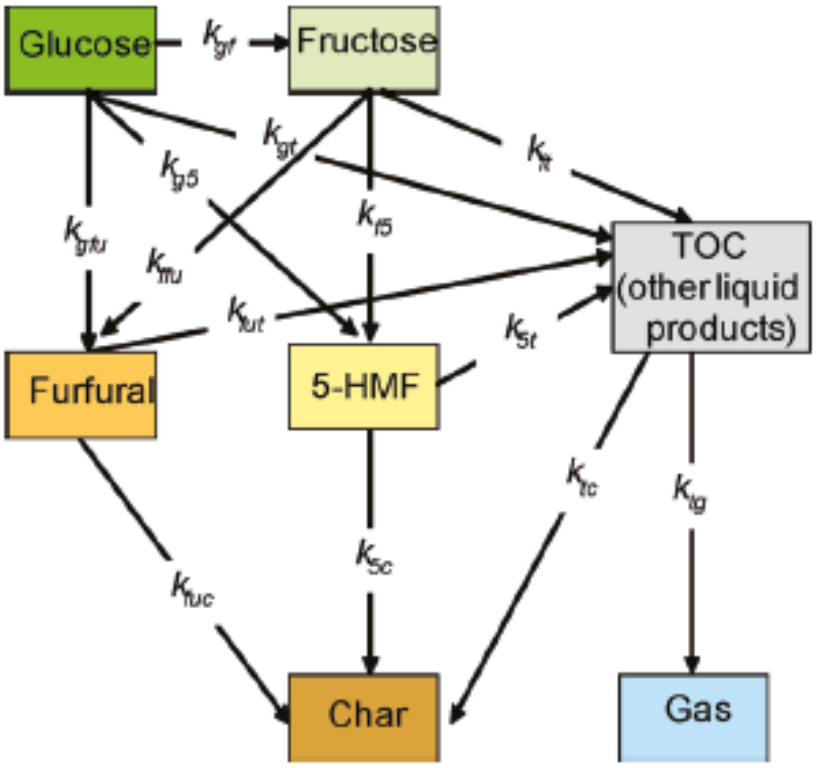

Fig. 4.16 reaction pathways of glucose gasification in supercritical water[14]

In order to complete the kinetic determination, those 4 chemicals were analyzed by using HPLC.

$$\frac{d[glucose]}{dt} = -(k_{gf} + k_{gfu} + k_{gfu} + k_{g5})[glucose] \quad (4.4)$$

$$\frac{d[fructose]}{dt} = k_{gf}[glucose] - (k_{f5} + k_{ffu} + k_{ft})[fructose] \quad (4.5)$$

$$\frac{d[5-HMF]}{dt} = k_{g5}[glucose] + k_{f5}[fructose] - k_{5t}[5-HMF] - k_{5c}[5-HMF] \quad (4.6)$$

$$\frac{d[furfural]}{dt} = k_{gfu}[glucose] + k_{ffu}[fructose] - (k_{fut} + k_{fuc})[furfural] \quad (4.7)$$

$$\frac{d[TOC]}{dt} = k_{gt}[glucose] + k_{ft}[fructose] + k_{5t}[5-HMF] + k_{fut}[furfural] - (k_{tc} + k_{tg})[TOC] \quad (4.8)$$

$$\frac{d[char]}{dt} = k_{fuc}[furfural] + k_{5c}[5-HMF] + k_{tc}[TOC] \quad (4.9)$$

$$\frac{d[gas]}{dt} = k_{tg}[TOC] \quad (4.10)$$

All products are represented by an amount of carbon in product divided by carbon in feedstock [-]. k_i is reaction rate constant [s^{-1}] and t is reaction time [s]. All the parameters were calculated using least squares error method by fitting the experimental data with the predicted value as shown in appendix D. The comparisons between experimental and predicted data were shown in **Fig. 4.17-4.19**.

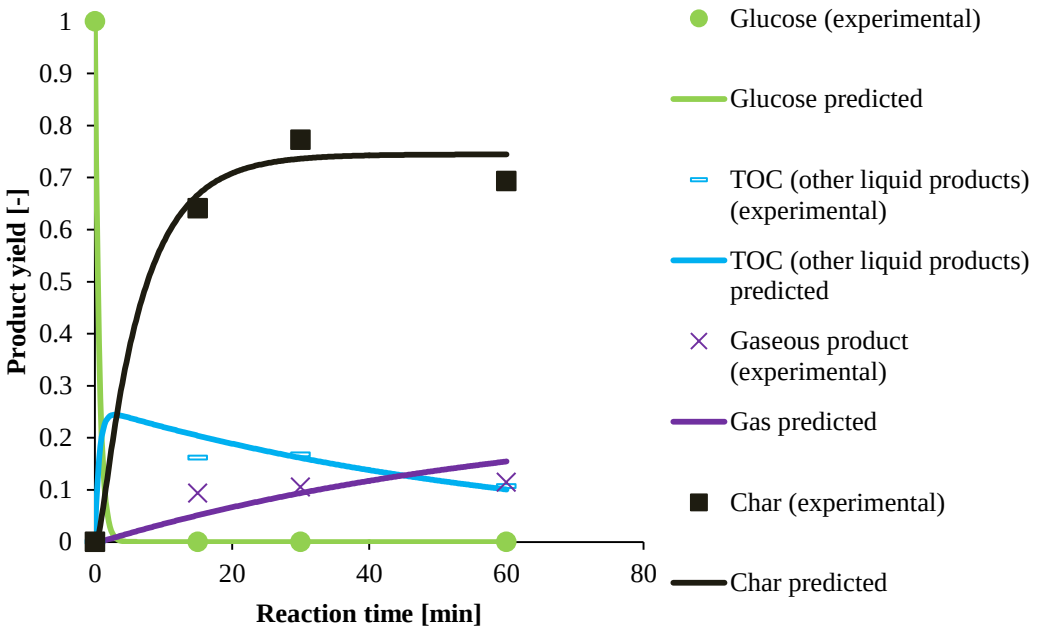

a) Glucose, TOC (other liquid products), gas, and char yields

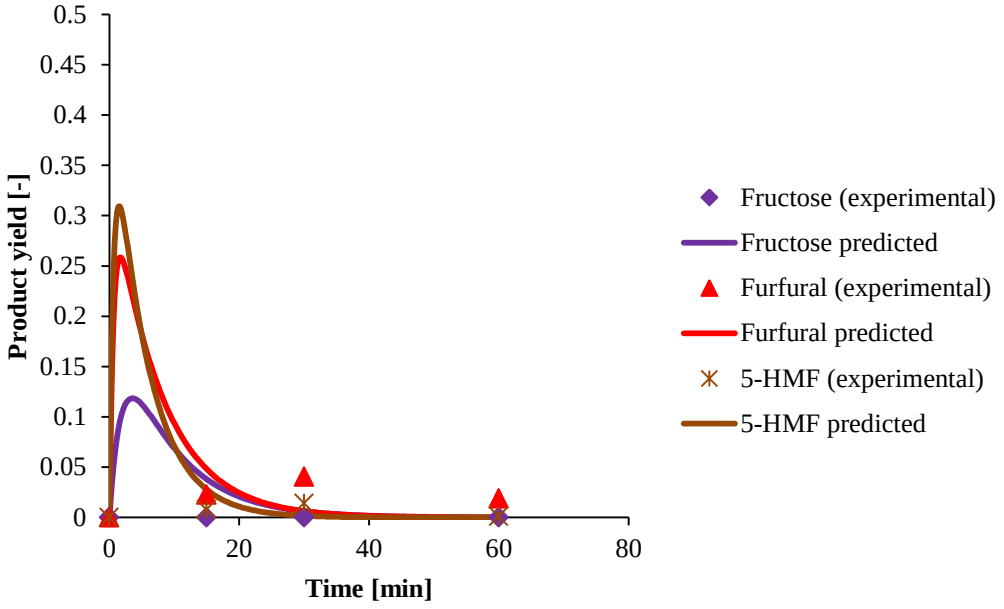

b) Fructose, furfural, and 5-HMF yields

Fig. 4.17 Comparisons between experimental and predicted yields from SWCNT-catalyzed SCWG of glucose at temperature of 400 °C and pressure of 25 MPa: a) glucose, TOC (other liquid products), gas, and char yields and b) fructose, furfural, and 5-HMF yields

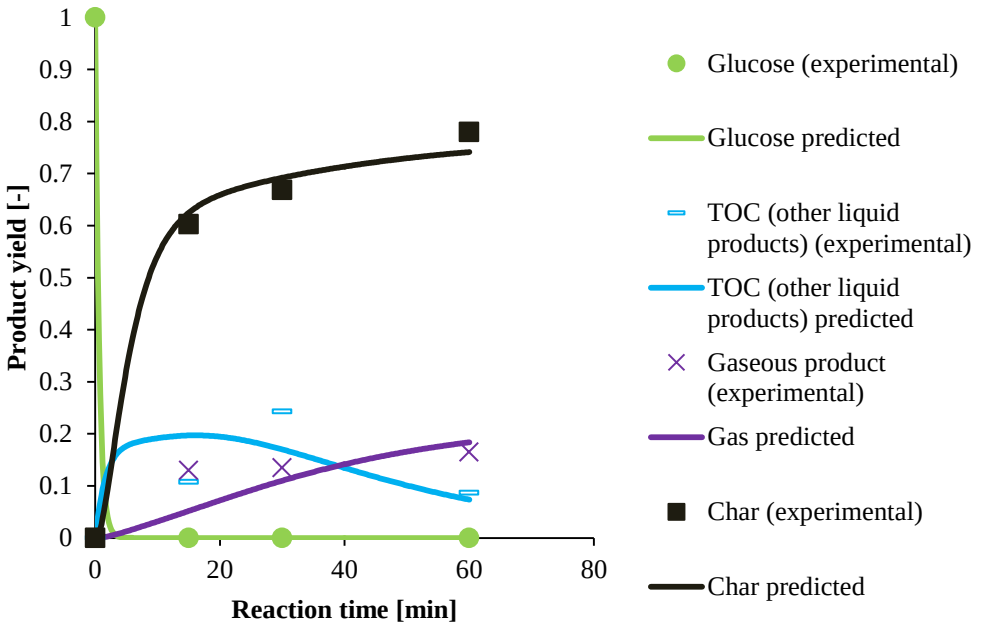

a) Glucose, TOC (other liquid products), gas, and char yields

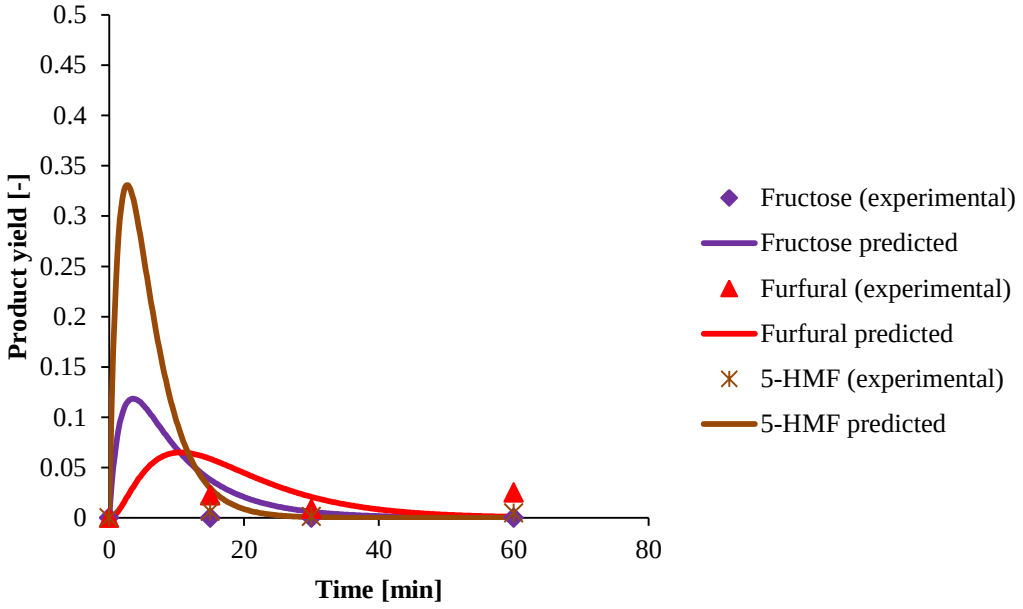

b) Fructose, furfural, and 5-HMF yields

Fig. 4.18 Comparisons between experimental and predicted yields from Ni/SWCNT-catalyzed SCWG of glucose at temperature of 400 °C and pressure of 25 MPa: a) glucose, TOC (other liquid products), gas, and char yields and b) fructose, furfural, and 5-HMF yields

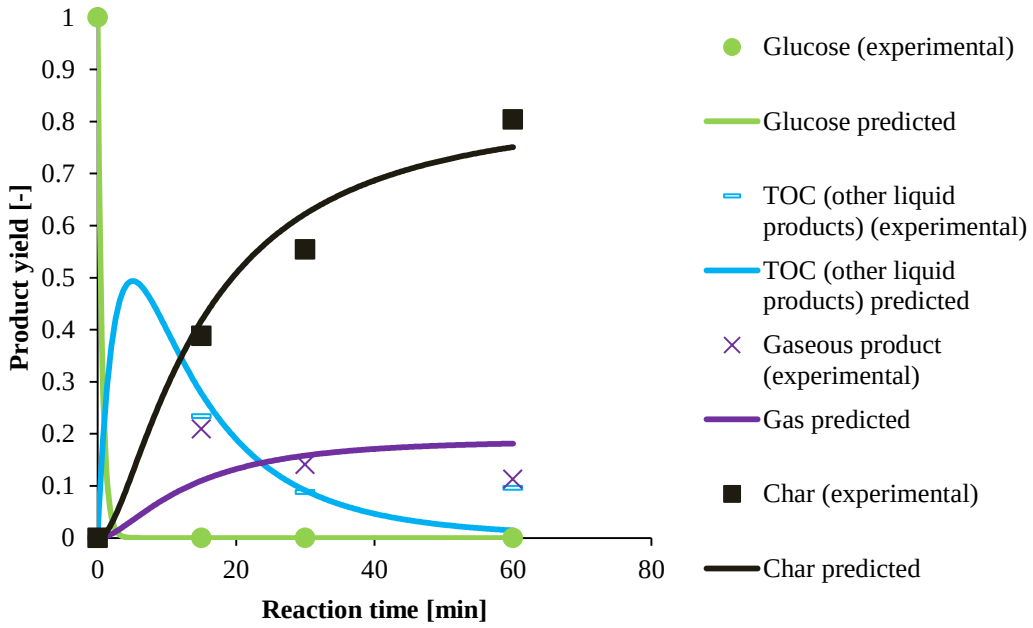

a) Glucose, TOC (other liquid products), gas, and char yields

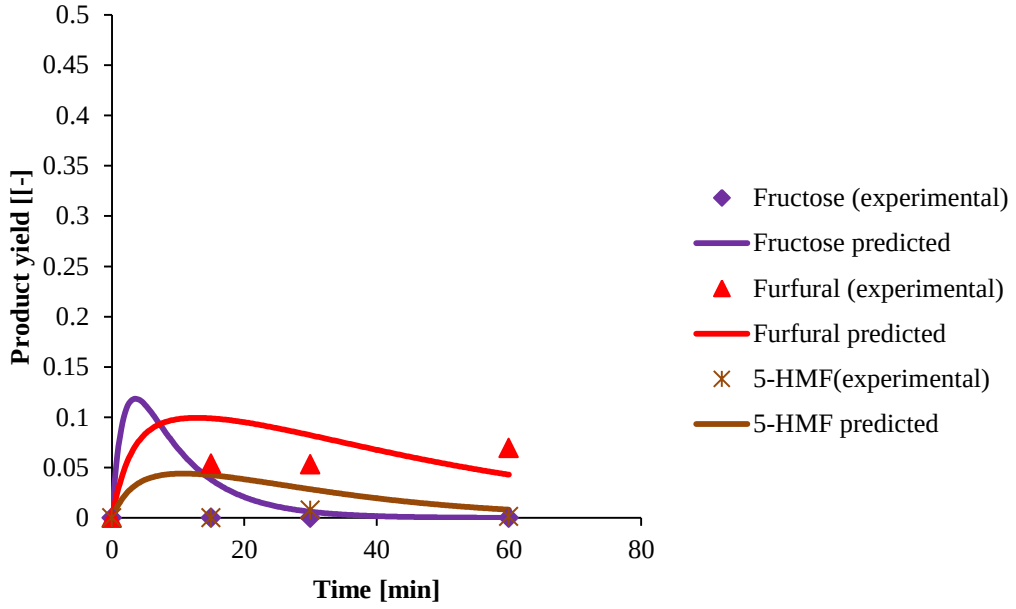

b) Fructose, furfural, and 5-HMF yields

Fig. 4.19 Comparisons between experimental and predicted yields from RuNi/SWCNT-catalyzed SCWG of glucose at temperature of 400 °C and pressure of 25 MPa: a) glucose, TOC (other liquid products), gas, and char yields and b) fructose, furfural, and 5-HMF yields

It can be seen from the predicted data that the important period of all reaction pathways was the very first period at reaction time below 10 min. At this period, reactions took place rapidly, suggesting that reactor performance in terms of heating rate has a great influence on gasification product of glucose in supercritical water because the undesirable products can be produced in low temperature region or under sub-critical water. At the reaction temperature lower than the critical point of water could enhance the polymerization product and other undesirable intermediates against gas production [16-17]. The rapid generation of furfural and 5-HMF which have been claimed to be the cause of increasing char product were demonstrated in Fig. 4.17-4.19. It can be noted that TOC (other liquid products) decreased slightly and then reacted to form gaseous product in the latter period of time. However, fructose cannot be found in liquid products. All of the reaction rate constants are shown in **Table 4.6**.

Table 4.6 Reaction rate constant

Parameters	**k [s^{-1}]**		
	SWCNT	Ni/SWCNT	Ru-Ni/SWCNT
gf	2.98×10^{-02}	9.26×10^{-02}	4.46×10^{-2}
gfu	4.39×10^{-01}	0	3.41×10^{-02}
gt	3.51×10^{-01}	1.02×10^{-01}	2.77×10^{-01}
g5	5.55×10^{-01}	3.19×10^{-01}	1.52×10^{-02}
f5	8.30×10^{-02}	0	3.14×10^{-02}
ffu	7.87×10^{-02}	$1.20\times10\text{-}^{01}$	3.97×10^{-02}
ft	0	0	0
5t	1.17×10^{-04}	0	4.38×10^{-02}
5c	1.90×10^{-01}	2.38×10^{-01}	9.74×10^{-03}
fut	0	1.20×10^{-01}	2.65×10^{-03}
fuc	1.36×10^{-01}	0	2.32×10^{-02}
tc	0	1.36×10^{-02}	6.69×10^{-02}
tg	$1.56\times10\text{-}^{02}$	2.06×10^{-02}	1.92×10^{-02}

It seemed that adding Ni-based catalyst can suppress some reactions including dehydration of glucose to furfural and fructose to 5-HMF, decomposition of fructose to TOC (other liquid products) and 5-HMF to TOC (other liquid products), and finally polymerization of furfural to char. When Ru and Ni were added together, the results showed that dehydration of glucose, and fructose, decomposition of 5-HMF, and

polymerization of furfural took place in the reactor as shown in Table 4.6. TOC (other liquid products) was rapidly produced in case of Ru-Ni/SWCNT because k_{gt} was much higher than Ni/SWCNT case. However, k_{tc} of Ni/SWCNT and Ru-Ni/SWCNT cases can be considered equal with a small difference between 2.06×10^{-02} and 1.92×10^{-02} s^{-1}. Consequently, gas production from Ru-Ni/SWCNT was significant at the first period of reaction while Ni/SWCNT gradually produced gaseous product with reaction time increase as shown in Fig. 4.18a and 4.19a.

CHAPTER V

CONCLUSION AND RECOMMENDATION

Glucose was gasified in supercritical water with various conditions. SWCNT, Ni/SWCNT, and Ru-Ni/SWCNT were synthesized by using impregnation, calcination, and reduction steps. BET analysis, EDX, XRD, TEM, were introduced to analyze the synthesized catalysts. Non-catalytic and catalytic gasification experiments were carried out by varying reaction times. As a result, carbon gasification efficiency obtained from non-catalytic gasification of glucose showed insignificant differences in a range of 9.95-11.37 %. When SWCNT was added, CGE insignificantly increased from 9.33 to 11.44 %, suggesting that there was no effect of supporting SWCNT on CGE. However, hydrogen content slightly increased from 5.70 to 18.55 vol% which was higher when compared to experiment with no catalyst. Ni/SWCNT resulted in a dramatic increase in hydrogen content from 8.48 to 34.03 vol% with reaction time increase. It can be noted that water-gas shift reaction was promoted with nickel catalyst resulting in hydrogen production. Furthermore, TOC yield decreased while char yield increased because TOC can undergo polymerization resulting in char production. When Ru-Ni/SWCNT was used as catalyst, hydrogen was rapidly produced in the first 15 min providing hydrogen content of 31.84 vol% and considerably increased to 35.08 and 43.70 vol% at 30 and 60 min, respectively.

Recommendation

All metal-based catalysts used in this study were reduced into Ru (0) and Ni (0) before supercritical water gasification of glucose. It would be more interesting if Ru and Ni are used with high oxidation state to understand and effect of oxidation state on product distribution. Moreover, effect of Ru should be investigate without Ni for better understanding of Ru-based catalyst.

REFERENCES

1. Yakaboylu, O., et al., *Supercritical Water Gasification of Biomass: A Literature and Technology Overview.* Energies, 2015. **8**(2): p. 859-894.
2. Rashidi, M. and A. Tavasoli, *Hydrogen rich gas production via supercritical water gasification of sugarcane bagasse using unpromoted and copper promoted Ni/CNT nanocatalysts.* The Journal of Supercritical Fluids, 2015. **98**: p. 111-118.
3. Zhang, L., P. Champagne, and C. Xu, *Supercritical water gasification of an aqueous by-product from biomass hydrothermal liquefaction with novel Ru modified Ni catalysts.* Bioresource Technology, 2011. **102**(17): p. 8279-8287.
4. Rodríguez-reinoso, F., *The role of carbon materials in heterogeneous catalysis.* Carbon, 1998. **36**(3): p. 159-175.
5. Akbayrak, S. and S. Ozkar, *Ruthenium(0) nanoparticles supported on multiwalled carbon nanotube as highly active catalyst for hydrogen generation from ammonia-borane.* ACS Appl Mater Interfaces, 2012. **4**(11): p. 6302-10.
6. Garcia, J., et al., *Carbon nanotube supported ruthenium catalysts for the treatment of high strength wastewater with aniline using wet air oxidation.* Carbon, 2006. **44**(12): p. 2384-2391.
7. Amuzu-Sefordzi, B., J. Huang, and M. Gong, *Hydrogen production by supercritical water gasification of food waste using nickel and alkali catalysts.* 2014. **1**: p. 285-296.
8. Furusawa, T., et al., *Hydrogen production from the gasification of lignin with nickel catalysts in supercritical water.* International Journal of Hydrogen Energy, 2007. **32**(6): p. 699-704.
9. Jin, H., et al., *Hydrogen Production by Supercritical Water Gasification of Biomass with Homogeneous and Heterogeneous Catalyst.* Advances in Condensed Matter Physics, 2014. **2014**: p. 1-9.
10. Azadi, P., et al., *Screening of nickel catalysts for selective hydrogen production using supercritical water gasification of glucose.* Green Chemistry, 2012. **14**(6): p. 1766.
11. Alonso, D.M., S.G. Wettstein, and J.A. Dumesic, *Bimetallic catalysts for upgrading of biomass to fuels and chemicals.* Chemical Society Reviews, 2012. **41**(24): p. 8075-8098.
12. Castello, D., A. Kruse, and L. Fiori, *Supercritical water gasification of glucose/phenol mixtures as model compounds for ligno-cellulosic biomass.* Chemical Engineering Transactions, 2014. **37**: p. 193-198.
13. Chuntanapum, A. and Y. Matsumura, *Char Formation Mechanism in Supercritical Water Gasification Process: A Study of Model Compounds.* Industrial & Engineering Chemistry Research, 2010. **49**(9): p. 4055-4062.
14. Promdej, C. and Y. Matsumura, *Temperature Effect on Hydrothermal Decomposition of Glucose in Sub- And Supercritical Water.* Industrial & Engineering Chemistry Research, 2011. **50**(14): p. 8492-8497.
15. Susanti, R.F., et al., *High-yield hydrogen production by supercritical water gasification of various feedstocks: Alcohols, glucose, glycerol and long-chain*

alkanes. Chemical Engineering Research and Design, 2014. **92**(10): p. 1834-1844.

16. Castello, D., A. Kruse, and L. Fiori, *Low temperature supercritical water gasification of biomass constituents: Glucose/phenol mixtures.* Biomass and Bioenergy, 2015. **73**: p. 84-94.
17. Watanabe, M., et al., *Glucose reactions within the heating period and the effect of heating rate on the reactions in hot compressed water.* Carbohydrate Research, 2005. **340**(12): p. 1931-1939.
18. Safari, F., et al., *Hydrogen and syngas production from gasification of lignocellulosic biomass in supercritical water media.* International Journal of Recycling of Organic Waste in Agriculture, 2015. **4**: p. 121-125.
19. David, S.C., W. Hay, and J. Pierce, *Biomass in the energy industry: an introduction.* 2014.
20. Schwarz, J.A., C. Contescu, and A. Contescu, *Methods for Preparation of Catalytic Materials.* Chemical Reviews, 1995. **95**(3): p. 477-510.
21. Azadi, P., et al., *Catalytic reforming of activated sludge model compounds in supercritical water using nickel and ruthenium catalysts.* Applied Catalysis B: Environmental, 2013. **134-135**: p. 265-273.
22. Osada, M., et al., *Low-Temperature Catalytic Gasification of Lignin and Cellulose with a Ruthenium Catalyst in Supercritical Water.* Energy & Fuels, 2004. **18**(2): p. 327-333.
23. Kaya, B., S.H. Irmak, A., and O. Erbatur, *Evaluation of various carbon materials supported Pt catalyts for aqueous-phase reforming of lignocellulosic biomass hydrolysate.* International Journal of Hydrogen Energy, 2014. **39**: p. 10135-10140.
24. Hu, Y.H. and E. Ruckenstein, *Pore size distribution of single-walled carbon nanotubes.* Industrial & Engineering Chemistry Research, 2004. **43**: p. 708-711.
25. Peigney, A., et al., *Specific surface area of carbon nanotubes and bundles of carbon nanotubes.* Carbon, 2001. **39**: p. 507-514.
26. Zhu, C., et al., *Effects of reaction time and catalyst on gasification of glucose in supercritical water: Detailed reaction pathway and mechanisms.* international Journal of Hydrogen Energy, 2016. **41**: p. 6630-6639.

APPENDIX A

Calibration curve of gas composition

Calibration curves of wanted gases had to be done. Firstly, air in gas bag was sucked out by using aspirator before filled with the hydrogen gas in case that GC-TCD system was being operated, while it was filled with carbon-containing gases (CO, CO_2, CH_4, C_2H_4, and C_2H_6) instead in case of GC-TCD-FID operation. That means this GC cannot be detected H2 and carbon-containing gases at each time. In order to make the calibration curve of each compound, 0.1, 0.2, and 0.3 ml of standard gas were injected in the GC injected port one by one by using syringe. The results were printed out by printer. Fig. A1-A7 show the examples of calibration curve made from standard gases. Finally, the sample was sucked out from the Vial for gas sample by using syringe. The injected volume was 0.3 ml for all samples.

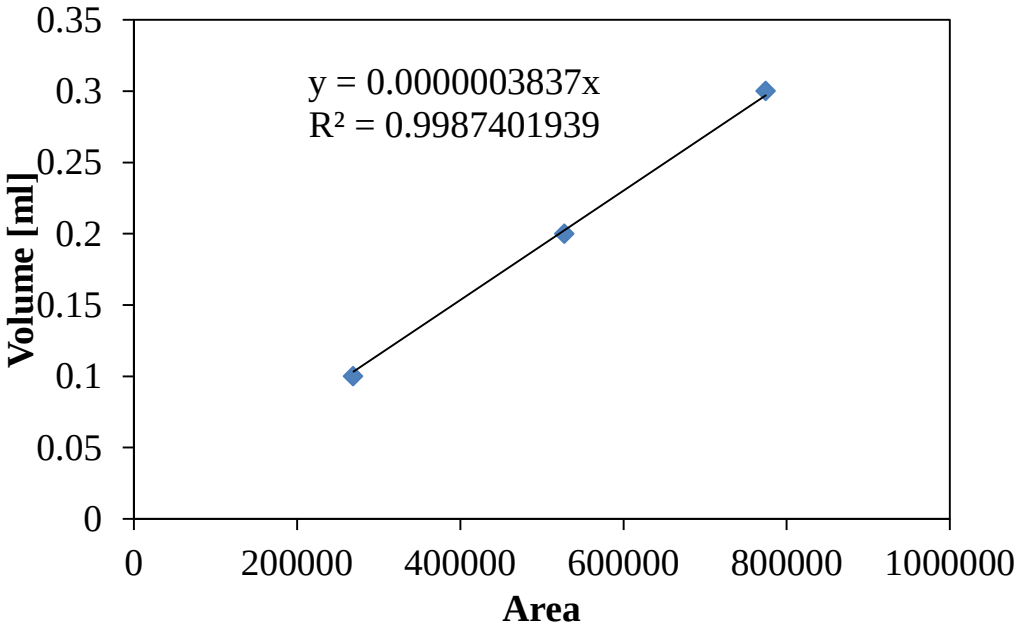

Fig. A1 Calibration curve of air in standard

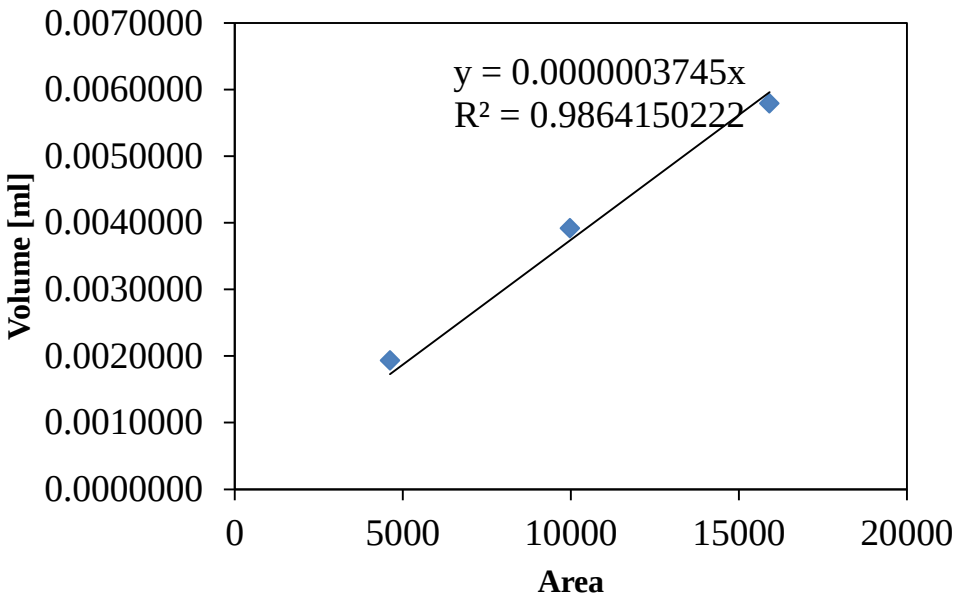

Fig. A2 Calibration curve of CO in standard

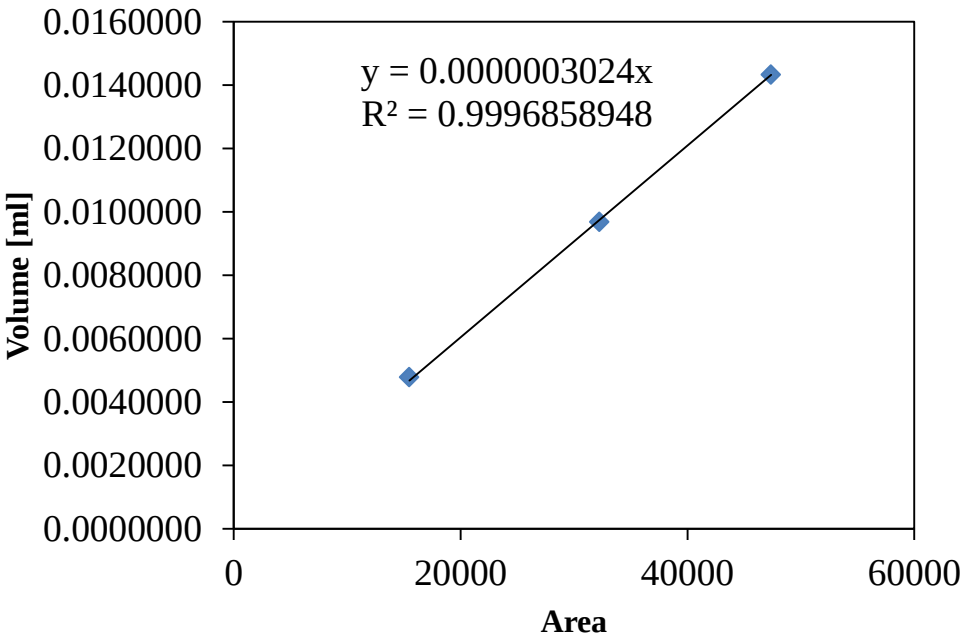

Fig. A3 Calibration curve of CO_2 in standard

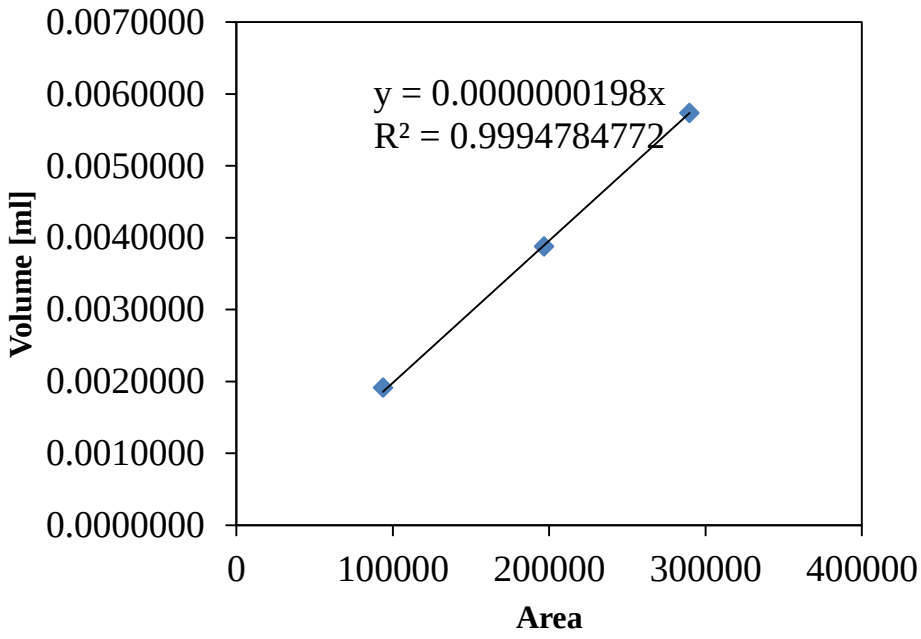

Fig. A4 Calibration curve of CH_4 in standard

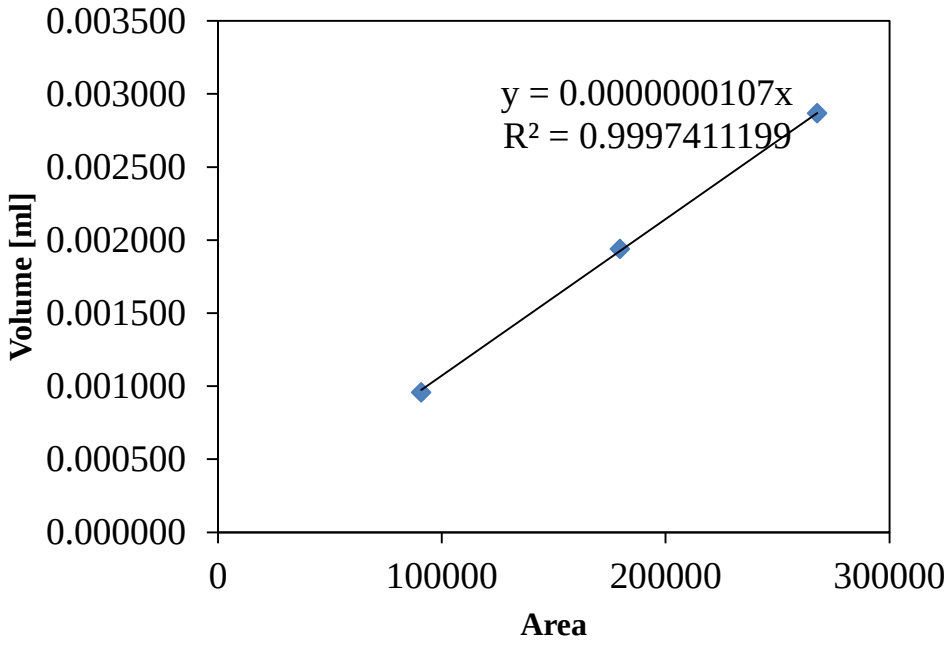

Fig. A5 Calibration curve of C_2H_4 in standard

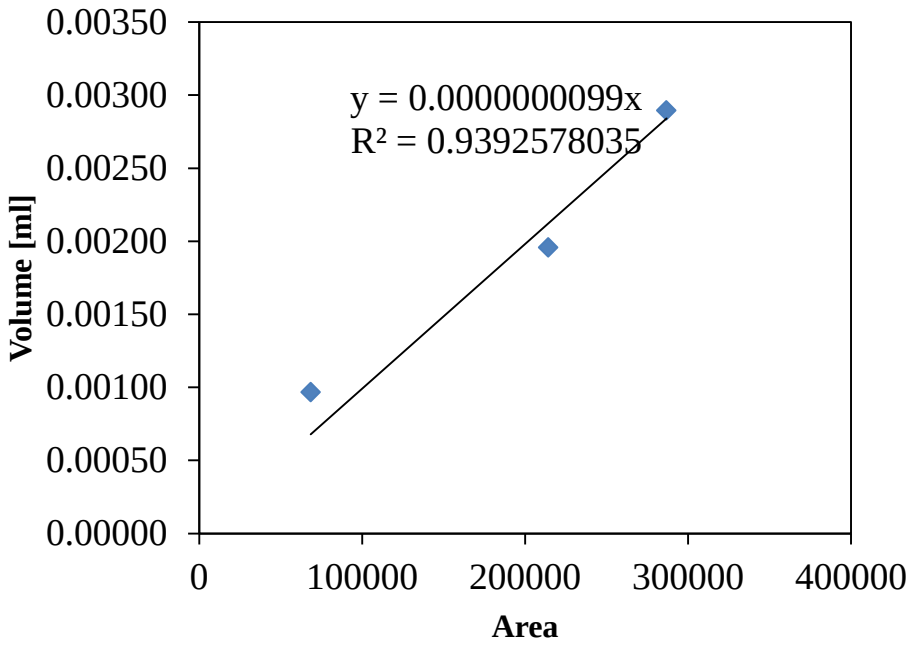

Fig. A6 Calibration curve of C_2H_6 in standard

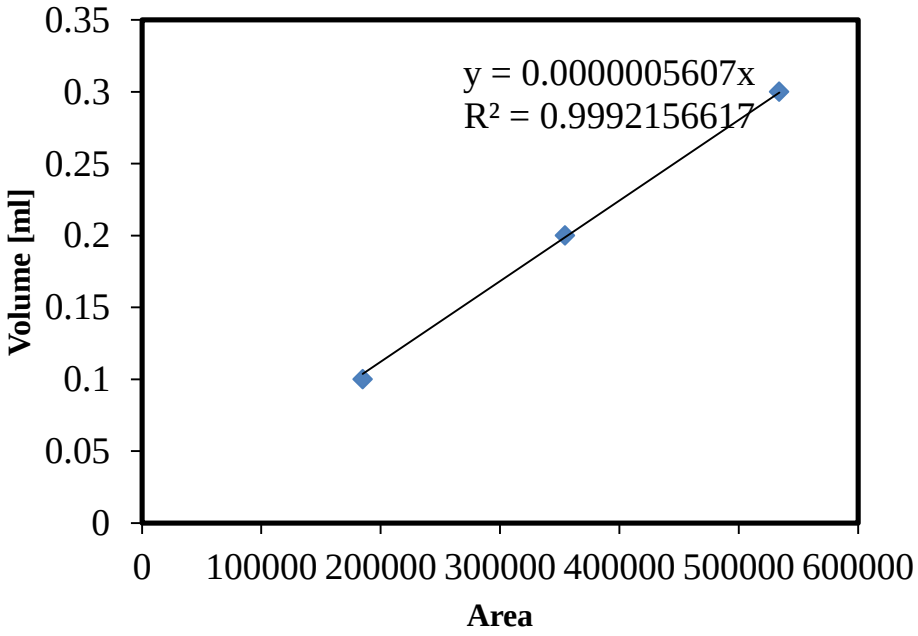

Fig. A7 Calibration curve of H_2 in standard

The equations obtained from Microsoft excel by plotting graph between volume injected and area of each peak. Finally, peak areas of each product were interpreted into volume out of 0.3 ml injected and calculated into vol %.

Carbon gasification efficiency or carbon yield of gaseous product can be obtained from the following equation.

$$\text{CGE}\ [-] = \frac{\text{carbon content in gaseoue product (mol C)}}{\text{carbon content in feedstock (mol C)}}$$

APPENDIX B

Total organic carbon analysis

TOC analyzer consists of sample port, computer, and printer. The sample was poured into the 25 ml-bottle and put in the sample port for analysis. The results showed 2 values consisting of non-purgeable organic carbon (NPOC) and inorganic carbon (IC). NPOC can refer to TOC while IC is included in gaseous product. Carbon yield in liquid product can be determined by using the following equation.

$$\text{Carbon yield}_{\text{liquid}} = \frac{\text{carbon content in liquid product (mol C)}}{\text{carbon content in feedstock (mol C)}}$$

APPENDIX C

Calibration curve of liquid product analyzed by HPLC

Calibration curves of glucose, fructose, 5-HMF, and furfural were made, as shown in Fig. C1-C4.

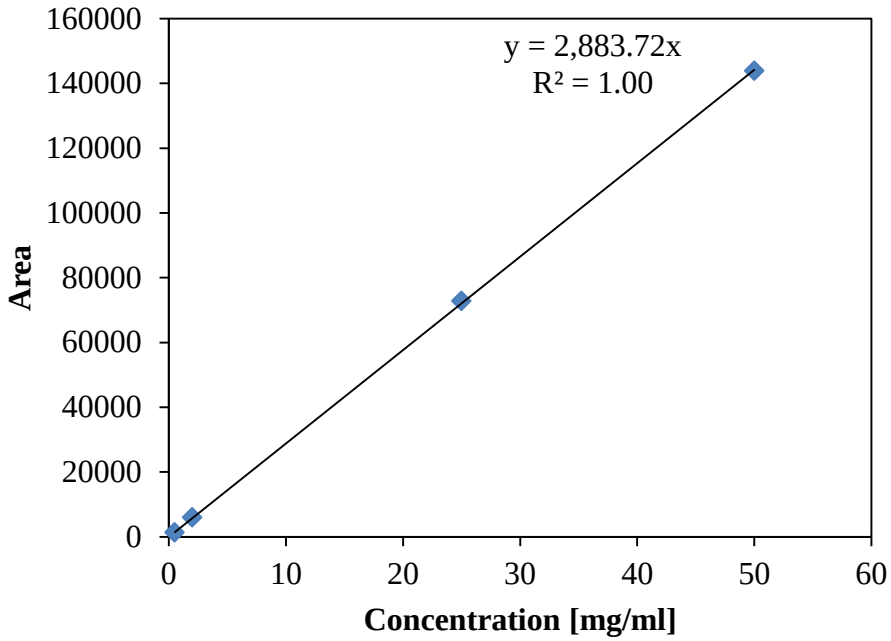

Fig. C1 Calibration curve of glucose

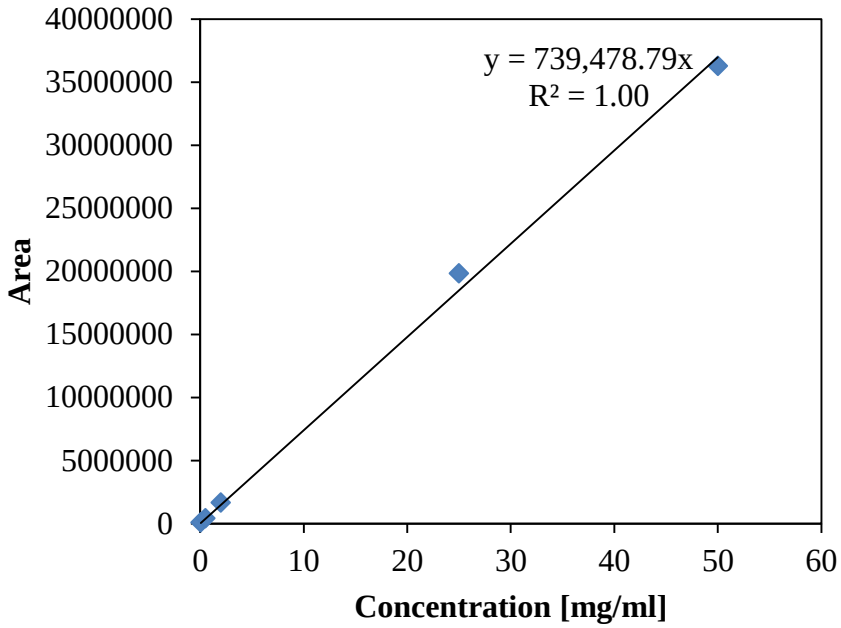

Fig. C2 Calibration curve of fructose

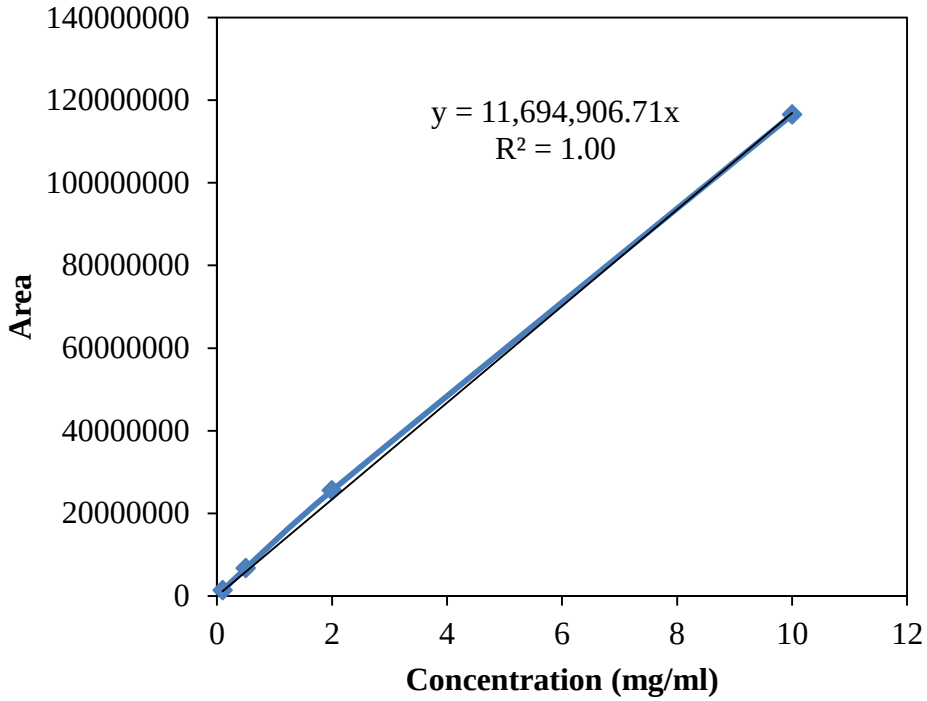

Fig. C3 Calibration curve of 5-HMF

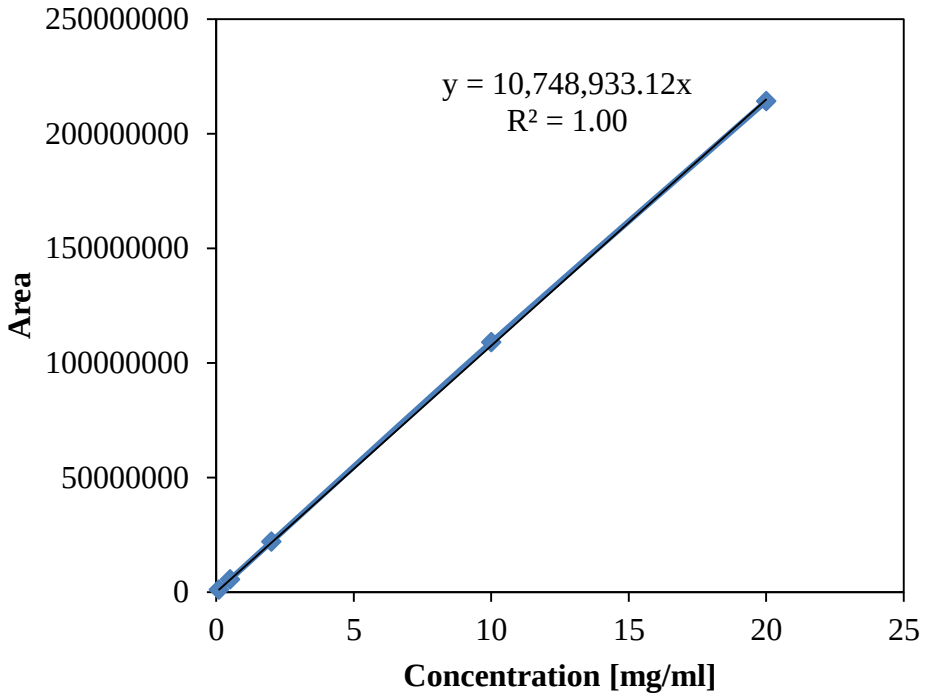

Fig. C4 Calibration curve of furfural

APPENDIX D

Calculation table for kinetic parameter determination

	Kinetic parameter (k)	
	qf	2.98E-02
	qfu	4.39E-01
	qt	3.51E-01
	q5	5.55E-01
	f5	8.30E-02
	ffu	7.87E-02
	ft	0.00E+00
	5t	1.17E-04
	5c	1.90E-01
	fut	0.00E+00
	fuc	1.36E-01
	tc	0.00E+00
	tq	1.56E-02
	q	1.109846092

Time (min)	Error						
	Glucose	Fructose	5-HMF	Furfural	TOC (De	Gas	Char
15	1.16803E-21	4.4E-06	0.000408474	0.00065	0.00181	0.001776695	0.00066
30	1.3643E-42	3.1E-08	0.000149868	0.00115	4.2E-05	0.000126543	0.00133
60	1.8613E-84	1.6E-12	8.51703E-07	0.00035	3.7E-05	0.00161103	0.00264

	Total error	0.01273

Experimental data								
	Product yield [-]							
Time (min)	Glucose	Fructose	5-HMF	Furfural	TOC	TOC (De	Gas	Char
0	1	0	0	0	0	0	0	0
15	0	0	0.007545912	0.02257	0.19186	0.16174	0.093319388	0.64109
30	0	0	0.01394731	0.04023	0.22208	0.16791	0.105208004	0.77277
60	0	0	0.000930187	0.01874	0.12666	0.10699	0.114387458	0.69307

Fig. D1 Example of calculation table of yields of products at each time with step size of 0.2 min from SWCNT-catalyzed SCWG of glucose at temperature of 400 °C and pressure of 25 MPa

Calculated data															
	Product yield [-]								d[Glucose	d[Fructos	d[5-HMF]	d[Furfural	d[TOC]	d[Gas]	d[Char]
Time (min)	Glucose	Fructose	5-HMF	Furfural	TOC	TOC (De	Gas	Char							
0	1	0	0	0	[redacted]	0	0	0	-0.27481	0.00597	0.11101	0.08772	0.07012	0	0
0.2	0.725186474	0.00597	0.111007713	0.08772		0.07012	0	0	-0.19929	0.00413	0.07638	0.06133	0.05063	0.00022	0.00659
0.4	0.525895422	0.0101	0.187390892	0.14904		0.12076	0.000219463	0.00659	-0.14452	0.00281	0.05143	0.04225	0.0365	0.00038	0.01115
0.6	0.381372247	0.01291	0.238818069	0.19129		0.15726	0.000597399	0.01775	-0.10481	0.00186	0.03348	0.02847	0.02626	0.00049	0.01425
0.8	0.276565995	0.01477	0.272295015	0.21976		0.18351	0.00108958	0.032	-0.076	0.00117	0.0206	0.01854	0.01883	0.00057	0.01629
1	0.200561919	0.01595	0.292896716	0.2383		0.20234	0.001663936	0.04829	-0.05512	0.00068	0.0114	0.01138	0.01344	0.00063	0.01758
1.2	0.14544479	0.01663	0.304298186	0.24968		0.21578	0.00229721	0.06587	-0.03997	0.00033	0.00486	0.00625	0.00953	0.00068	0.01832
1.4	0.105474595	0.01696	0.309159393	0.25594		0.22531	0.002972539	0.08419	-0.02899	8.1E-05	0.00025	0.00258	0.0067	0.00071	0.01867
1.6	0.076488749	0.01704	0.309404404	0.25852		0.232	0.003677697	0.10287	-0.02102	-9.5E-05	-0.00298	-2.9E-05	0.00464	0.00073	0.01875
1.8	0.055468606	0.01694	0.306423796	0.25849		0.23665	0.004403818	0.12162	-0.01524	-0.00022	-0.0052	-0.00187	0.00316	0.00074	0.01864
2	0.040225083	0.01673	0.301221452	0.25661		0.23981	0.005144477	0.14026	-0.01105	-0.0003	-0.0067	-0.00316	0.00208	0.00075	0.01839
2.2	0.029170686	0.01642	0.294520993	0.25345		0.24188	0.005895012	0.15866	-0.00802	-0.00036	-0.00768	-0.00405	0.0013	0.00076	0.01805
2.4	0.021154187	0.01607	0.286842963	0.2494		0.24318	0.006652049	0.17671	-0.00581	-0.00039	-0.00828	-0.00465	0.00073	0.00076	0.01765
2.6	0.01534073	0.01567	0.278560798	0.24475		0.24391	0.00741314	0.19436	-0.00422	-0.00042	-0.00862	-0.00504	0.00032	0.00076	0.01721
2.8	0.01112489	0.01526	0.2699414	0.23971		0.24423	0.008176513	0.21157	-0.00306	-0.00043	-0.00877	-0.00528	2.2E-05	0.00076	0.01675
3	0.00806762	0.01483	0.261174565	0.23442		0.24425	0.008940883	0.22831	-0.00222	-0.00043	-0.00878	-0.00541	-0.00019	0.00076	0.01627
3.2	0.005850529	0.0144	0.252394309	0.22901		0.24406	0.009705323	0.24458	-0.00161	-0.00043	-0.0087	-0.00547	-0.00035	0.00076	0.01579
3.4	0.004242724	0.01397	0.243694335	0.22354		0.24371	0.01046916	0.26037	-0.00117	-0.00043	-0.00856	-0.00547	-0.00046	0.00076	0.01531
3.6	0.003076766	0.01354	0.235139241	0.21808		0.24325	0.011231909	0.27569	-0.00085	-0.00042	-0.00837	-0.00543	-0.00054	0.00076	0.01484
3.8	0.002231229	0.01312	0.226772643	0.21265		0.24271	0.01199322	0.29052	-0.00061	-0.00041	-0.00815	-0.00536	-0.0006	0.00076	0.01437
4	0.001618057	0.01271	0.218623063	0.20729		0.24211	0.01275284	0.3049	-0.00044	-0.0004	-0.00791	-0.00528	-0.00064	0.00076	0.01392
4.2	0.001173393	0.01231	0.210708193	0.20201		0.24147	0.013510589	0.31882	-0.00032	-0.00039	-0.00767	-0.00518	-0.00067	0.00076	0.01348
4.4	0.000850929	0.01192	0.203037982	0.19683		0.2408	0.014266338	0.33229	-0.00023	-0.00038	-0.00742	-0.00507	-0.00069	0.00075	0.01304
4.6	0.000617082	0.01154	0.195616871	0.19176		0.24011	0.015019995	0.34534	-0.00017	-0.00037	-0.00717	-0.00496	-0.0007	0.00075	0.01262
4.8	0.0004475	0.01117	0.188445413	0.1868		0.23941	0.015771495	0.35796	-0.00012	-0.00036	-0.00692	-0.00485	-0.00071	0.00075	0.01222

Fig. D2 Example of calculation table of yields of products at each time with step size of 0.2 min from SWCNT-catalyzed SCWG of glucose at temperature of 400 °C and pressure of 25 MPa

By using Microsoft excel 2010 to calculate the kinetic parameters, all of product changes at each reaction time from 0 to 60 min can be done by arbitrarily setting step size of 0.2 min. the calculated product yields obtained from 0, 15, 30, and 60 min were compared to the experimental product yields to give errors defined as equation D-1. The minimum summation of errors was given by using solver function. So, the best appropriate fitting parameters were achieved as shown in Fig. D1-D2.

$$(\text{Experimental yield} - \text{predicted yield})^2 = \text{error} \qquad \text{(D-1)}$$

VITA

I was born in Bangkok in 1992. I went to elementary school named Sang Arun School when I was 7 years old. I entered high school named Taweethapisek School. When I was 18 years old, I received admittance to study undergraduate in Kasetsart University. I have decided to study chemical engineering. In the last year, of undergraduate student life, I have chosen to conduct my research in a theme of bioenergy. Producing biofuel from black liquor which is waste from paper-producing industry was the topic. I can successfully got Bachelor degree in Chemical Engineering in 2014. In that year, I have decided to continually study Master degree in Chemical Engineering in Chulalongkorn University with Assoc. Prof. Tawatchai Charinpanitkul as my advisor. He is a Professor in Center of Excellence in Particle Technology. After 1 year of master student life, my advisor and Prof. Yukihiko Matsumura, who is a professor in Faculty of Engineering, Division of Energy and Environmental Engineering, Hiroshima University, gave me an opportunity to be a research student in Hiroshima University for around 1 year. I got a lot of salary from The New Energy and Industrial Technology Development Organization (NEDO) to conduct research about converting shochu residue into gaseous product which was a claasified project. I also received scholarship from Hiroshima University to conduct research which is a part of my final thesis in Chulalongkorn University as can be seen in this thesis. Moreover, I also got scholarship from Thailand Graduate Institute of Science and Technology (TGIST) which have provided me tuition fee and living expense.